CLIMATE FEEDBACKS

Drought-induced peatland carbon loss exacerbated by elevated CO_2 and warming

Quan Quan[1]†, Jian Zhou[1]†, Paul J. Hanson[2], Daniel Ricciuto[2], Stephen D. Sebestyen[3], David J. Weston[4], Jeffrey P. Chanton[5], Rachel M. Wilson[5], Joel E. Kostka[6], Yu Zhou[7], Ning Wei[1], Lifen Jiang[1], Melanie A. Mayes[2], Jonathan M. Stelling[2], Andrew D. Richardson[8,9], Mirindi Eric Dusenge[10], Danielle Way[10,11,12], Jeffrey M. Warren[2], Yiqi Luo[1]*

Extreme drought events are predicted to increase with climate change, yet their impacts on ecosystem carbon dynamics under warming and elevated carbon dioxide (eCO_2) remain unclear. In a peatland experiment with five warming treatments each under ambient carbon dioxide (aCO_2) and eCO_2 (+500 parts per million), a 2-month extreme drought in 2021 reduced net ecosystem productivity by 444.0 ± 65.8 and 736.6 ± 57.8 grams of carbon per square meter at +9°C under aCO_2 and eCO_2, respectively—228.6 ± 56.8% and 381.9 ± 83.4% of the reduction at +0°C under aCO_2. This exacerbation was driven by warming-induced water table decline, prolonged low water tables, and CO_2-enhanced substrate availability through increased plant carbon inputs. Findings indicate that future climate will greatly amplify carbon loss during extreme drought, reinforcing positive carbon-climate feedbacks.

The latest Intergovernmental Panel on Climate Change (IPCC) report projects extreme drought events to become 1.7 to 7.2 times more frequent if the surface temperature increases by 4°C in the near future (*1*). Studies examining the effects of extreme drought under current climates (*2*–*7*) suggest that more frequent extreme drought events have the potential to substantially affect ecosystem carbon (C) cycling. For example, Ciais *et al.* reported a 30% decline in gross primary productivity over Europe during the 2003 European summer drought, resulting in a net C release of 0.5 Pg C $year^{-1}$, which is equivalent to 4 years of C sequestration under nondrought conditions (*8*). Similarly, Wolf *et al.* found that the 2012 US summer drought reduced net ecosystem productivity (NEP) by 0.23 Pg C per season throughout the United States, with a 71% reduction in the Great Plains, United States (*9*). These severe impacts represent large-scale declines in plant growth and increased mortality (*4*, *5*), which can offset ecosystem C sinks and even reverse them into C sources across both time and space (*3*, *5*, *10*–*13*). Such disruptions could intensify positive climate-C feedback, accelerating future warming (*14*, *15*). However, how extreme drought events will influence NEP in a future world with higher temperatures and elevated carbon dioxide (eCO_2) concentration remains unclear.

Field experiments offer opportunities to study the impacts of extreme drought events on ecosystem C processes under future climate scenarios (*16*, *17*). For example, during experimental warming that increased soil temperature by up to 2.6°C and air temperature by 1.1°C in a tallgrass prairie of the Great Plains from 1999 to 2019, an extreme drought event in 2011 reduced NEP by 23.5% under ambient temperature but 53.5% under warming with clipping (*18*). In a temperate peatland ecosystem, an extreme summer drought event in 2018 reduced NEP by approximately 57.8% compared with a nondrought year (2020) under ambient temperature and by around 146.2% under +3.2°C warming (*19*). In addition to warming, eCO_2 is another key driver of future climates. Numerous studies in upland ecosystems have shown that eCO_2 can mitigate the negative drought impacts on ecosystem C sequestration by stimulating photosynthesis (*20*–*22*), conserving water (*21*, *23*, *24*), and improving plant water-use efficiency (*22*, *25*). However, to the best of our knowledge, no studies have examined the impacts of naturally occurring extreme drought events on NEP in a field experiment combining eCO_2 and warming in peatland or other ecosystems (*26*).

Peatlands, although covering only 3% of the land surface, store around 500 billion tonnes (Gt) C (nearly one-third of the world's soil C or about half of the C stored in the atmosphere) because of waterlogging conditions that inhibit decomposition (*27*–*29*). Climate warming driven by eCO_2 and associated extreme events pose a great threat to peatland C sequestration (*30*–*32*). Understanding how the large peatland C stocks respond to extreme drought events under combined warming and eCO_2 is essential so that we can accurately predict the global C budget and future climate. To study peatland response to future climate scenarios, the Spruce and Peatland Responses Under Changing Environments (SPRUCE) project was established as a long-term field experiment that has five whole-ecosystem warming levels (+0°, +2.25°, +4.5°, +6.75°, and +9°C) each under two CO_2 levels (ambient and +500 parts per million) in a northern boreal peatland in Minnesota, United States. The warming gradients were designed to capture the upper limit (8.3° ± 1.9°C) of projected high-latitude warming under Representative Concentration Pathway 8.5 (RCP8.5) by 2100 (*33*).

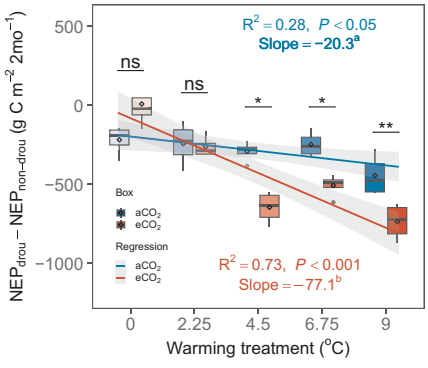

Fig. 1. Effects of extreme drought on NEP under different warming and CO_2 scenarios. NEP_{drou} and $NEP_{non\text{-}drou}$ represent NEP in the 2 months (July and August) in drought year 2021 and nondrought years, respectively. The lower and upper boundaries of the boxplots indicate the 25th and 75th quartiles. The center lines indicate the median values, the rhombus-shaped points inside the boxes indicate the mean values, and the whiskers indicate 1.5 times the interquartile range (IQR). The fitted lines indicate regressions, and the shaded bands indicate 95% confidence intervals (CIs). Different letters denote significantly different slopes. *P* values were adjusted by using the Benjamini-Hochberg false discovery rate correction for multiple comparisons. Differences between aCO_2 and eCO_2 under each warming treatment are ns, not significant; $*P < 0.05$; $**P < 0.01$.

[1]Soil and Crop Sciences Section, School of Integrative Plant Science, Cornell University, Ithaca, NY, USA. [2]Environmental Sciences Division, Oak Ridge National Laboratory, Oak Ridge, TN, USA. [3]Northern Research Station, Forest Service, US Department of Agriculture (USDA), Grand Rapids, MN, USA. [4]Biosciences Division, Oak Ridge National Laboratory, Oak Ridge, TN, USA. [5]Department of Earth, Ocean and Atmospheric Science, Florida State University, Tallahassee, FL, USA. [6]School of Biological Sciences, Georgia Institute of Technology, Atlanta, GA, USA. [7]Department of Environmental Systems Science, ETH Zurich, Zurich, Switzerland. [8]Center for Ecosystem Science and Society, Northern Arizona University, Flagstaff, AZ, USA. [9]School of Informatics, Computing, and Cyber Systems, Northern Arizona University, Flagstaff, AZ, USA. [10]Division of Plant Science, Research School of Biology, The Australian National University, Canberra, Australia. [11]Department of Biology, The University of Western Ontario, London, ON, Canada. [12]Nicholas School of the Environment, Duke University, Durham, NC, USA. ***Corresponding author. Email: yl2735@cornell.edu** †These authors contributed equally to this work.

An extreme drought event at the SPRUCE site in 2021 (July–August) substantially lowered the water table to levels below the 10th percentile of the historical range from 1961 to 2021 (fig. S1). The average water table during this period was 411.93 m above sea level, close to the lowest record of 411.82 m during the same period in 1976, the driest year since 1961. This drought lowered the water table depth (WT) by 0.24 m on average in the control plot [+0°C under ambient CO_2 (aCO_2)], which is consistent with reported declines of 0.2 to 0.3 m in other northern peatlands during extreme drought events (*34*–*36*). Taking advantage of this concurrence of a peatland warming and eCO_2 experiment with an extreme drought event in 2021, we explored the response of peatland NEP to the natural extreme drought event under five warming and two CO_2 levels. We hypothesize that (i) an extreme drought event and warming promote reduction in NEP, likely by exacerbating water table drawdown, increasing soil aeration, and enhancing microbial decomposition, and (ii) eCO_2 offsets the NEP reduction, potentially buffering the C loss under extreme drought and warming.

Effects of extreme drought on NEP under warming and eCO_2

The extreme 2-month drought (July and August) in 2021 significantly reduced NEP by 217.9 ± 46.4 g C m^{-2} (mean ± SE) ($P < 0.05$) at ambient temperature and aCO_2 in comparison with that in nondrought years (2016–2019) (no measurement was made in 2020 because of the COVID-19 pandemic) (Fig. 1). This drought effect is comparable in magnitude with the annual NEP declines (range, 218 to 234 g C m^{-2}) reported in other northern peatlands because most of these annual losses occurred during the drought period (*37*, *38*). At ambient temperature and eCO_2, the NEP insignificantly increased by 8.6 ± 79.4 g C m^{-2} ($P > 0.05$) (Fig. 1) during the drought event, likely because of enhanced water-use efficiency and photosynthesis under eCO_2 offsetting the negative impact of drought (*22*, *25*, *26*, *39*). However, at +9°C, the drought event caused a notable decrease in NEP by 444.0 ± 65.8 g C m^{-2} ($P < 0.01$) under aCO_2 and 736.6 ± 57.8 g C m^{-2} ($P < 0.01$) under eCO_2 over 2 months compared with NEP in the nondrought years (Fig. 1). The NEP response to the extreme drought under warming and eCO_2 was primarily due to increased ecosystem respiration (ER). Both of the factors (warming and eCO_2) significantly amplified the drought-induced increase in ER (fig. S2, A and B). Specifically, ER increased by 513.7 ± 44.0 g C m^{-2} ($P < 0.01$) under aCO_2 and 651.7 ± 98.1 g C m^{-2} ($P < 0.01$) under eCO_2 at +9°C during this extreme drought compared with that in the nondrought years.

Mechanisms driving amplified C loss under eCO_2 during drought

The difference in drought effects on NEP between aCO_2 and eCO_2 was significantly negatively correlated with drought-induced changes in number of days with WT below −0.25 m (Fig. 2 and table S1). As shown in fig. S3, significant correlations emerged only when the water table fell below −0.25 m, suggesting it as a critical threshold for strong C flux response to drought. This aligns with the range of −0.2 to −0.3 m that is reported for other peatlands where C cycling is strongly affected (*40*–*43*). In addition, drought-induced declines in WT and increases in vapor pressure deficit (VPD) led to greater increases in ER under eCO_2 (fig. S4 and table S2). eCO_2 could amplify the increase in ER induced by water table decline by enhancing the supply of labile C from leaf litterfall and root exudation (*44*–*46*), which facilitate decomposition, and by accelerating belowground C turnover (*47*, *48*). Globally, eCO_2 significantly increases leaf and root biomass by 21 and 45%, respectively; increases microbial biomass by 21%; and stimulates soil respiration by nearly 30% (*47*). At the SPRUCE site, we also found increased plant-derived C substrates under eCO_2. Before the eCO_2 treatment started in 2014, peat soil carbohydrate concentrations were similar between plots assigned to aCO_2 and eCO_2 treatments. However, they increased significantly in the eCO_2 plots after 4 years of eCO_2 treatment in 2019 ($P < 0.01$) (Fig. 3), averaging 33.7% compared with 28.7% under aCO_2 across the soil profile to a depth of 2 m. Moreover, hydrolysable biopolymers increased by nearly 20% under eCO_2 after 2 years of the eCO_2 treatment (*49*), which may contribute to the overall 5% increase in carbohydrate content and higher porewater CO_2 concentrations under eCO_2 across the peat soil profile, at depths of up to 2 m (Fig. 3) (*50*). Thus, as drought deepened the water table, more C substrates accumulated under eCO_2 became exposed to oxygen, leading to increased CO_2 release through respiration.

As the number of days with WT below −0.25 m increased, the effect of eCO_2 on the impact of drought on gross ecosystem productivity changed from mitigation to exacerbation (fig. S5 and table S3), reflecting a dependence on drought duration, which in our study was mainly driven by the warming treatments. Under a short-term drought condition, eCO_2 generally enhances photosynthesis and water-use efficiency while delaying stomatal closure, allowing plants to maintain higher C uptake (amplified CO_2 fertilizer effect) (*25*, *39*, *51*). However, prolonged severe drought can impair stomatal function and photosynthetic

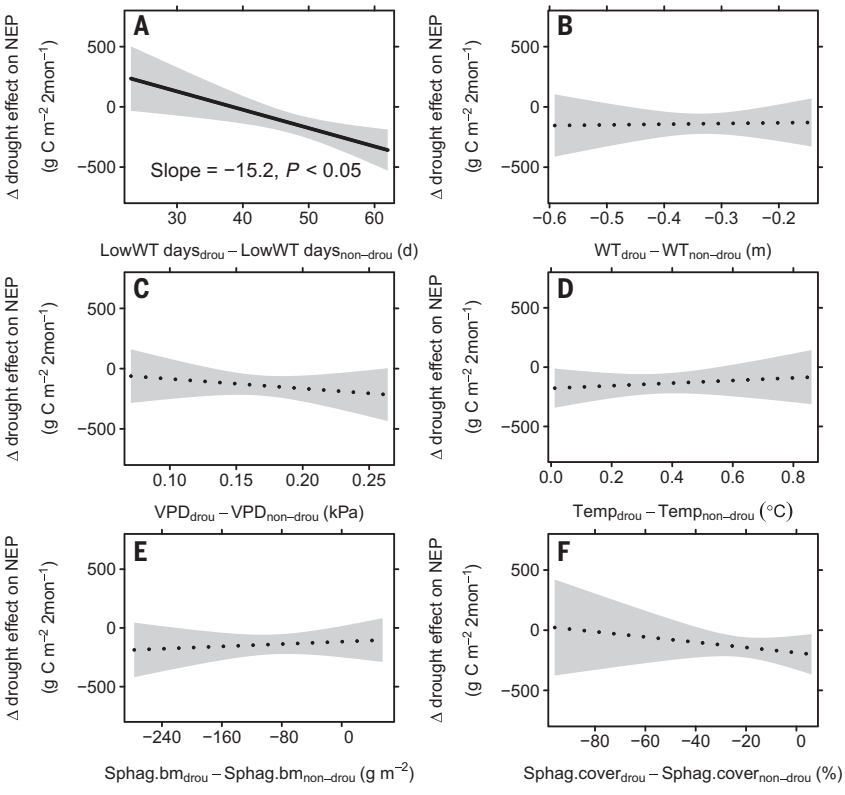

Fig. 2. Difference in drought effects on NEP between aCO_2 and eCO_2 treatment as related to various predictors. The difference, denoted by Δdrought effect on NEP, depends on drought-induced changes in (**A**) number of low-water-table (LowWT, below −0.25 m) days, (**B**) WT, (**C**) VPD, (**D**) temperature (Temp), (**E**) *Sphagnum* biomass (Sphag.bm), and (**F**) *Sphagnum* coverage (Sphag.cover), respectively. The fitted lines indicate the estimated effect of each predictor while controlling all other predictors. Solid lines indicate significant effects, and dashed lines indicate insignificant effects, with a significance level set at $\alpha = 0.05$. The shaded bands indicate 95% CIs.

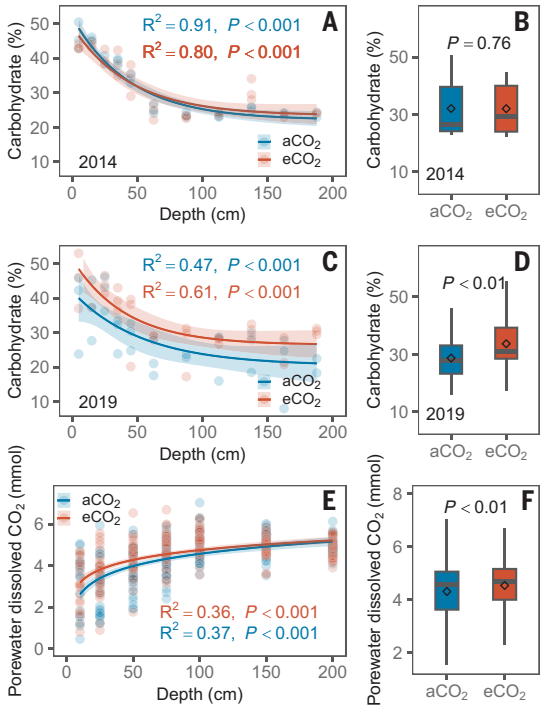

Fig. 3. Carbohydrate and porewater dissolved CO_2 concentrations in peat soil under aCO_2 and eCO_2. (**A** to **D**) Depth profiles of carbohydrate concentrations in [(A) and (B)] 2014 (before the eCO_2 treatment) and [(C) and (D)] 2019 (after the eCO_2 treatment). (**E** and **F**) Depth profile of porewater dissolved CO_2 concentrations between aCO_2 and eCO_2. The lower and upper boundaries of the boxplots indicate the 25th and 75th quartiles. The center lines indicate the median values, the rhombus-shaped points inside the boxes indicate the mean values, and the whiskers indicate 1.5 times the IQR. The fitted lines indicate regressions, and the shaded areas indicate 95% CIs.

structures (*52*). In such conditions, eCO_2-induced premature leaf senescence and abscission, along with excessive stomatal closure, can intensify the negative impact of drought on C uptake (*53*, *54*). Ridge regression analysis, which accounts for collinearity among drought-induced changes in all these potential causal variables (the number of low-water-table days, WT, VPD, temperature, and *Sphagnum* biomass and coverage), further supported these results (fig. S6). The differences in C flux responses to drought between aCO_2 and eCO_2 were not caused by differential drought responses of these factors because these responses were similar (figs. S7 and S8) and did not significantly differ between the two CO_2 treatments (figs. S9 to S11). Overall, with greater water table decline and an increased number of days with low water table, warming and eCO_2 jointly promote C release and suppress C uptake, exacerbating the decline in NEP during extreme drought.

Mechanisms driving amplified C loss under warming during drought

Under both CO_2 treatments, warming significantly amplified the drought-induced reductions in NEP. The temperature sensitivity of this response was 77.1 g C m^{-2} $°C^{-1}$ under eCO_2, which is significantly greater than the 20.3 g C m^{-2} $°C^{-1}$ under aCO_2 ($P < 0.001$) (Fig. 1). Warming can directly exacerbate peatland C loss during drought by shifting plant and soil fungal communities and enhancing the activity of C-degrading enzymes, which stimulates decomposition of recalcitrant deeper peat, as shown in many studies (*30*, *55*–*57*). Under nondrought conditions, it has been estimated that a 1°C increase in temperature reduces NEP by 17.0 [95% confidence interval (CI): 8.0 to 26.0] g C m^{-2} $year^{-1}$ across 16 northern peatland sites, which is comparable with the 24.6 (95% CI: 17.6 to 33.5) g C m^{-2} $year^{-1}$ reduction observed in the SPRUCE site (*58*). In addition, warming strongly amplifies drought-induced water table decline (fig. S9), exposing more peat to aerobic decomposition. A study showed that a water table decline of >0.3 m can strongly accelerate microbial respiration by 123% across global boreal peatlands (*43*). In our study, although warming did not significantly alter drought's effects on other variables (figs. S10 and S11), it significantly enhanced the water table decline and the number of low-water-table days during drought (fig. S9). Further analysis showed that warming-aggregated water table decline significantly contributed to warming-amplified increase in ER and decrease in NEP during drought (fig. S12). Moreover, warming promotes substrate availability for microbial decomposition in peatlands (*57*, *59*, *60*), which in combination with drought further accelerates peat soil C loss. Specifically, at the SPRUCE site, warming strongly promoted shrub fine-root growth by 1.2 km m^{-2} $year^{-1}$ $°C^{-1}$ in 2016 and by 2.54 km m^{-2} $°C^{-1}$ during the growing season (June to October) of 2017 (*61*). Increased belowground C allocation and root-derived labile metabolites primarily contributed to peat C release under warming (*31*, *49*, *50*, *62*). All of these processes will lead peatlands to lose more C under warming during extreme drought events.

Implications

These findings support our first hypothesis that warming intensifies peatland C loss during extreme drought events by enhancing microbial decomposition and lowering the water table. However, contrary to our second hypothesis, eCO_2, which typically mitigates drought impacts in upland ecosystems, exacerbated C loss in peatland by providing more substrate for decomposition and suppressing C assimilation under extreme drought and warming (*44*–*47*, *53*, *54*, *60*, *63*–*66*). The exacerbated peatland C loss during extreme drought under warming and eCO_2 (228.6 ± 56.8% and 381.9 ± 83.4% of the control at +9°C under aCO_2 and eCO_2, respectively) far exceeds that observed under current climates. This suggests that peatland C sinks may become increasingly vulnerable to future climate extremes.

In this study, the extreme drought period was defined on the basis of ambient water table dynamics. Whereas ambient plots exhibited water table drawdown and recovery during this period, warming plots experienced deeper and more prolonged water table drawdown without recovery during this period, likely because of higher VPD and evapotranspiration. This divergence explains the greater C loss under warming and eCO_2, underscoring that future droughts and their impacts could be much more severe than under the current climate. Our current analysis excluded NEP responses during the recovery phase under warming because it extended beyond the extreme window defined by ambient conditions. If the water table recovery phases were considered, the delayed recovery phases may cause more C loss under warming and eCO_2. Therefore, the recovery phase warrants further investigation (*10*, *26*).

Whether the warming- and eCO_2-amplified drought effects on C loss are short- or long-term remains an open question. Drought temporarily increases aerobic conditions, enhancing decomposition. However, when the water table recovers, peat returns to anaerobic conditions that slow decomposition. Moreover, much of the labile C may have already been decomposed during drought, potentially limiting post-drought decomposition. If drought persists, shifts in plant communities and organic C inputs could introduce new feedbacks that alter photosynthesis and decomposition over longer timescales (*67*, *68*). Whereas our short-term observations show that warming and eCO_2 immediately amplified C loss under extreme drought, the long-term impacts will depend on ecosystem responses to drought duration, frequency, and the combined effects of warming and eCO_2 (*67*, *68*).

Undisturbed northern peatlands are weak net C sinks, with long-term C accumulation rates ranging from 3 to 80 g C m^{-2} $year^{-1}$ over

the past millennium (*69*), which is comparable with the 8 to 82 g C m^{-2} $year^{-1}$ measured at the SPRUCE site (*70*, *71*). This short-term NEP loss during the extreme drought event at +9°C under eCO_2 would erase 9.0 to 92.1 years of net C accumulation at the SPRUCE site, or potentially 9.2 to 245.5 years in other northern peatlands. Our study did not quantify drought impacts on methane (CH_4) emissions because it accounts for only a small fraction (7%) of ecosystem C exchange in northern peatlands (*72*) and typically approaches zero under drought condition when the water table drops to approximately −0.2 to approximately −0.3 m (*42*, *67*, *73*). Thus, it likely contributes little to net C loss during extreme drought. Consistent evidence from peatland studies shows that the increased CO_2 emission in response to drought and water table drawdown overwhelmingly outweighed the cooling effect from a reduction in CH_4 production, yielding a net warming effect (*42*, *74*, *75*). As extreme drought events become more frequent, our findings suggest that episodic C losses during the short-term droughts may substantially undermine long-term peatland C sequestration under future climate scenarios and pose a greater threat to the global C balance than current climate-based projections suggest.

REFERENCES AND NOTES

1. IPCC, *Climate Change 2021: The Physical Science Basis. Contribution of Working Group I to the Sixth Assessment Report of the Intergovernmental Panel on Climate Change*, V. Masson-Delmotte *et al.*, Eds. (Cambridge Univ. Press, 2021).
2. B. D. Stocker *et al.*, *Nat. Geosci.* **12**, 264–270 (2019).
3. A. Bastos *et al.*, *Sci. Adv.* **6**, eaba2724 (2020).
4. E. Martínez-García *et al.*, *Nat. Geosci.* **17**, 197–204 (2024).
5. A. C. Bennett *et al.*, *Nat. Clim. Chang.* **13**, 967–974 (2023).
6. D. Gampe *et al.*, *Nat. Clim. Chang.* **11**, 772–779 (2021).
7. Q. Quan *et al.*, *Sci. Adv.* **5**, eaav1131 (2019).
8. P. Ciais *et al.*, *Nature* **437**, 529–533 (2005).
9. S. Wolf *et al.*, *Proc. Natl. Acad. Sci. U.S.A.* **113**, 5880–5885 (2016).
10. C. Werner *et al.*, *Science* **374**, 1514–1518 (2021).
11. Y. Yang *et al.*, *Nat. Commun.* **9**, 3172 (2018).
12. J. Liu *et al.*, *Sci. Adv.* **10**, eadl2201 (2024).
13. O. L. Phillips *et al.*, *Science* **323**, 1344–1347 (2009).
14. M. Reichstein *et al.*, *Nature* **500**, 287–295 (2013).
15. D. Frank *et al.*, *Glob. Chang. Biol.* **21**, 2861–2880 (2015).
16. S. Sippel *et al.*, *Curr. Clim. Change Rep.* **4**, 266–286 (2018).
17. J. Song *et al.*, *Nat. Ecol. Evol.* **3**, 1309–1320 (2019).
18. C. G. Jung *et al.*, *Agric. For. Meteorol.* **276-277**, 107635 (2019).
19. S. Salimi, M. Berggren, M. Scholz, *Glob. Chang. Biol.* **27**, 5154–5168 (2021).
20. K. E. Mueller *et al.*, *Ecol. Lett.* **19**, 956–966 (2016).
21. J. A. Morgan *et al.*, *Nature* **476**, 202–205 (2011).
22. P. M. A. Fransson *et al.*, *New Phytol.* **152**, 431–442 (2001).
23. J. Radolinski *et al.*, *Science* **387**, 290–296 (2025).
24. S. Leuzinger, C. Körner, *Glob. Change Biol.* **13**, 2498–2508 (2007).
25. Z. Wang, C. Wang, S. Liu, *J. Ecol.* **110**, 2836–2849 (2022).
26. J. Roy *et al.*, *Proc. Natl. Acad. Sci. U.S.A.* **113**, 6224–6229 (2016).
27. J. Limpens *et al.*, *Biogeosciences* **5**, 1475–1491 (2008).
28. P. Friedlingstein *et al.*, *Earth Syst. Sci. Data* **15**, 5301–5369 (2023).
29. Z. Yu, J. Loisel, D. P. Brosseau, D. W. Beilman, S. J. Hunt, *Geophys. Res. Lett.* **37**, 2010GL043584 (2010).
30. E. Dorrepaal *et al.*, *Nature* **460**, 616–619 (2009).
31. A. L. Gill, M. A. Giasson, R. Yu, A. C. Finzi, *Glob. Chang. Biol.* **23**, 5398–5411 (2017).
32. S. Page *et al.*, *Nat. Rev. Earth Environ.* **3**, 426–443 (2022).
33. IPCC, *Climate Change 2013: The Physical Science Basis. Contribution of Working Group I to the Fifth Assessment Report of the Intergovernmental Panel on Climate Change*, T. F. Stocker *et al.*, Eds. (Cambridge Univ. Press, 2013).
34. M. Lund, T. R. Christensen, A. Lindroth, P. Schubert, *Environ. Res. Lett.* **7**, 045704 (2012).
35. J. Bubier, P. Crill, A. Mosedale, S. Frolking, E. Linder, *Global Biogeochem. Cycles* **17**, 2002GB001946 (2003).
36. T. Ise, A. L. Dunn, S. C. Wofsy, P. R. Moorcroft, *Nat. Geosci.* **1**, 763–766 (2008).
37. R. Garisoain *et al.*, *J. Geophys. Res. Biogeosci.* **129**, e2024JG008041 (2024).
38. C. Estop-Aragonés, K. Zając, C. Blodau, *Glob. Chang. Biol.* **22**, 2285–2300 (2016).
39. E. A. Ainsworth, S. P. Long, *Glob. Chang. Biol.* **27**, 27–49 (2021).
40. N. Fenner, C. Freeman, *Nat. Geosci.* **4**, 895–900 (2011).
41. D. Olefeldt *et al.*, *Glob. Chang. Biol.* **23**, 2428–2440 (2017).
42. C. D. Evans *et al.*, *Nature* **593**, 548–552 (2021).
43. L. Ma *et al.*, *Commun. Earth Environ.* **3**, 254 (2022).
44. S. Q. Wan, R. J. Norby, K. S. Pregitzer, J. Ledford, E. G. O'Neill, *New Phytol.* **162**, 437–446 (2004).
45. R. B. Jackson, C. W. Cook, J. S. Pippen, S. M. Palmer, *Ecology* **90**, 3352–3366 (2009).
46. C. A. Dietzen *et al.*, *Glob. Chang. Biol.* **25**, 2970–2977 (2019).
47. J. Cui *et al.*, *Nat. Clim. Chang.* **14**, 511–517 (2024).
48. M. Jiang *et al.*, *Nature* **580**, 227–231 (2020).
49. N. O. E. Ofiti *et al.*, *Nat. Commun.* **14**, 7533 (2023).
50. R. M. Wilson *et al.*, *Proc. Natl. Acad. Sci. U.S.A.* **118**, e2004192118 (2021).
51. S. Li, X. Li, Z. Wei, F. Liu, *Curr. Opin. Plant Biol.* **56**, 174–180 (2020).
52. L. O. A. Abdelhakim, R. Zhou, C.-O. Ottosen, *Agronomy (Basel)* **12**, 2526 (2022).
53. J. M. Warren, R. J. Norby, S. D. Wullschleger, *Tree Physiol.* **31**, 117–130 (2011).
54. M. G. De Kauwe, B. E. Medlyn, D. T. Tissue, *New Phytol.* **231**, 2118–2124 (2021).
55. A. Asemaninejad, R. G. Thorn, B. A. Branfireun, Z. Lindo, *Soil Biol. Biochem.* **120**, 28–36 (2018).
56. A. M. Hopple *et al.*, *Nat. Commun.* **11**, 2373 (2020).
57. L. Bragazza, J. Parisod, A. Buttler, R. D. Bardgett, *Nat. Clim. Chang.* **3**, 273–277 (2013).
58. M. Helbig *et al.*, *Nat. Clim. Chang.* **12**, 743–749 (2022).
59. A. Volder, R. M. Gifford, J. R. Evans, *Phalaris Glob. Change Biol.* **13**, 1040–1052 (2007).
60. K. Meeran *et al.*, *Glob. Chang. Biol.* **27**, 3230–3243 (2021).
61. A. Malhotra *et al.*, *Proc. Natl. Acad. Sci. U.S.A.* **117**, 17627–17634 (2020).
62. R. M. Wilson *et al.*, *Nat. Commun.* **7**, 13723 (2016).
63. O. C. Calvo *et al.*, *Glob. Chang. Biol.* **23**, 1292–1304 (2017).
64. L. Xiong *et al.*, *Soil Biol. Biochem.* **159**, 108289 (2021).
65. Y. Carrillo, F. Dijkstra, D. LeCain, D. Blumenthal, E. Pendall, *Ecol. Lett.* **21**, 1639–1648 (2018).
66. N. O. E. Ofiti *et al.*, *Glob. Chang. Biol.* **28**, 883–898 (2022).
67. S. Frolking *et al.*, *Environ. Rev.* **19** (NA), 371–396 (2011).
68. S. E. Ward *et al.*, *Ecol. Lett.* **16**, 1285–1293 (2013).
69. A. V. Gallego-Sala *et al.*, *Nat. Clim. Chang.* **8**, 907–913 (2018).
70. P. J. Hanson *et al.*, *AGU Adv.* **1**, e2020AV000163 (2020).
71. N. A. Griffiths *et al.*, *Soil Sci. Soc. Am. J.* **81**, 1668–1688 (2017).
72. Z. C. Yu, *Biogeosciences* **9**, 4071–4085 (2012).
73. H. Chen, X. Xu, C. Fang, B. Li, M. Nie, *Nat. Clim. Chang.* **11**, 766–771 (2021).
74. Y. Huang *et al.*, *Nat. Clim. Chang.* **11**, 618–622 (2021).
75. A. Günther *et al.*, *Nat. Commun.* **11**, 1644 (2020).
76. Q. Quan *et al.*, Drought-induced peatland carbon loss exacerbated by elevated CO_2 and warming. figshare (2024); https://doi.org/10.6084/m9.figshare.27857655.
77. Oak Ridge National Laboratory, SPRUCE: Spruce and Peatland Responses Under Changing Environments. https://mnspruce.ornl.gov/ (n.d.).

ACKNOWLEDGMENTS

We thank the SPRUCE program and team for supporting this study. We thank the many researchers who contributed data to the SPRUCE project database. **Funding:** This research was conducted under the Terrestrial Ecosystem Sciences Scientific Focus Area at Oak Ridge National Laboratory (ORNL), a program funded by the US Department of Energy (DOE), Office of Science, and the Office of Biological and Environmental Research. ORNL operates under the management of UT-Battelle for the DOE under contract DE-AC05-1008 000R22725. The contributions from Y.L. EcoLab at Cornell University were supported in part by funding from the US National Science Foundation (NSF; grants DEB 2242034, DEB 2406930, and DEB 2425290), as well as by the DOE's Terrestrial Ecosystem Sciences Grant (DESC0023514). Additional support was provided through the "NYS Connects: Climate Smart Farms & Forestry" project, funded collaboratively by the US Department of Agriculture (USDA), the New York State Department of Environmental Conservation, and the New York State Department of Agriculture and Markets. This work is also part of the AI Institute for Land, Economy, Agriculture and Forestry (AI-LEAF), supported by the USDA National Institute of Food and Agriculture (NIFA) and the NSF National AI Research Institutes Competitive Award (2023-67021-39829). Contributions by J.E.K., J.P.C., and R.M.W. were supported in part by the Office of Biological and Environmental Research, Genomic Science Program, under DOE contract DE-SC0023297). Contributions and long-term monitoring by S.D.S. at the Marcell Experimental Forest were supported by the USDA Forest Service, Northern Research Station. Contributions by D.W. were supported by the Natural Sciences and Engineering Research Council of Canada (NSERC) Strategic Project Grant STPGP 521445-18. **Author contributions:** Conceptualization: Y.L. and Q.Q. Project administration: P.J.H. Data curation: P.J.H. Investigation: P.J.H., S.D.S., D.J.W., J.P.C., R.M.W., J.E.K., M.A.M., J.M.S., A.D.R., M.E.D., D.W., and J.M.W. Visualization: Q.Q., J.Z., and Y.L. Writing – original draft: Q.Q., J.Z., and Y.L. Writing – review & editing: Q.Q., P.J.H., D.R., S.D.S., D.J.W., J.P.C., R.M.W., J.E.K., J.M.W., J.Z., Y.Z., N.W., L.J., M.A.M., J.M.S., A.D.R., M.E.D., D.W., and Y.L. **Competing interests:** The authors declare that they have no competing interests. **Data and materials availability:** All data and code used in this paper have been deposited in figshare (https://doi.org/10.6084/m9.figshare.27857655) (*76*). All the datasets are also cited in the materials and methods and publicly available in the online SPRUCE project archive at http://mnspruce.ornl.gov (*77*).

SUPPLEMENTARY MATERIALS

science.org/doi/10.1126/science.adv7104
Materials and Methods; Figs. S1 to S17; Tables S1 to S3; References (*78*–*124*);
MDAR Reproducibility Checklist

Submitted 7 January 2025; accepted 9 September 2025

10.1126/science.adv7104

Science
AAAS

Supplementary Materials for

Drought-induced peatland carbon loss exacerbated by elevated CO_2 and warming

Quan Quan *et al*.

Corresponding author: Yiqi Luo, yl2735@cornell.edu

Science **390**, 367 (2025)
DOI: 10.1126/science.adv7104

The PDF file includes:

Materials and Methods
Figs. S1 to S17
Tables S1 to S3
References

Other Supplementary Material for this manuscript includes the following:

MDAR Reproducibility Checklist

Materials and Methods

Study site

The Spruce and Peatland Responses Under Climatic and Environmental Change (SPRUCE) experiment was conducted at the S1 bog within the USDA Forest Service Marcell Experimental Forest (MEF) in northern Minnesota, USA, situated at approximately 47° 30' N and 93° 27' W, with an elevation of 418 m above mean sea level. The climate of the MEF is characterized as subhumid continental. Over the past 60 years, the mean annual air temperature was 3.3°C, rising at a rate of about 0.4°C per decade (*78*). The average annual precipitation was 779 mm from 1961 to 2021 at this site (*79*). The study site is dominated by two tree species: *Picea mariana* (Mill.) Britton, Sterns, and Poggenburg (black spruce) and *Larix laricina* (Du Roi) K. Koch (tamarack). The understory is mainly comprised of shrubs including *Rhododendron groenlandicum* (Oeder) Kron and Judd (labrador tea) and *Chamaedaphne calyculata* (L.) Moench. (leatherleaf), along with herbaceous species *Maianthemum trifolium* (L.) Sloboda, *Carex* spp. and *Eriophorum vaginatum*. Vegetation within the site includes a bryophyte layer dominated by *Sphagnum* spp., such as *S. divinum*, *S. angustifolium*, and *S. fallax* (*80, 81*). The peat is a Greenwood series, Typic Haplohemist, with average depths of 2-3 m (*82, 83*). The accumulated C storage exceeds 240 kg C m^{-2}, with over 90% of it dating back more than 3000 years (*80, 83*).

Experimental design

Whole-ecosystem warming began August 2015, while the belowground-only warming was initiated in 2014. The elevated CO_2 (eCO_2) treatment started in June 2016. Whole-ecosystem warming occurs in open-top enclosures with a dimension of 12.8 m in diameter × 7 m in height. Air and soil are warmed at five levels: +0°C, +2.25°C, +4.5°C, +6.75°C, and +9°C. To achieve air warming, four propane-fired furnaces generate warm air from recirculated air within each enclosure since 2015. A portion of warmed air is recaptured and routed back to the air handing ductwork via 4 air intake diffusers. Peat is warmed using an array of 67 low wattage, 3-m long resistance heaters inside coated pipe emplaced throughout the enclosed plot since 2014. Targeting the enclosure plot peat volume, 19 belowground heaters only add heat energy at peat depths from -2 to -3 m, avoiding direct heating of the measured peat profiles. Temperature control points were established at 2 m aboveground for air temperature and 2 m belowground for soil temperature.

To represent a high end of predicted atmospheric CO_2 scenario by the end of this century (*80*), atmospheric CO_2 concentration is elevated to 900 ppm in the eCO_2 plots (exceeding CO_2 concentrations in 2016 by +500 ppm) since 2016. The CO_2 source (Praxair, Inc.) is obtained from fossil fuel-based fertilizer plants. Pure CO_2 is distributed and mixed within the air handling manifolds prior to additions into each enclosure. Both horizontal and vertical mixing processes within each enclosure ensure homogenization of air, effectively distributing the added CO_2 with the heated air.

Overall, there are 10 enclosures. Two enclosures were constructed for each temperature treatment and one with ambient CO_2 concentration and the other received the eCO_2 treatment. Warming occurs throughout the year, while elevated CO_2 treatment is applied only during daylight hours of the growing season. Detailed information on the eCO_2 and warming treatments can be found in (*84*) and (*80*).

Biotic and abiotic variables measurement

Water table depth (WT) was recorded every half-hour using water level probes (Trutrack Ltd. Christchurch, New Zealand; Part No. WT-VO2000) placed in a 5.25 cm diameter well casing. Peat temperatures were recorded every 30 minutes by multipoint thermistor probes (W.H. Cooke and Co. Inc, Hanover, PA) up to 2 m below ground within each plot. Air temperatures at 2 m above the

peat surface were measured using a combination sensor (Vaisala, Finland; Model HMP155A) at the center of each plot. Vapor pressure deficit (VPD) was calculated using a function of air temperature and relative humidity. All the data sets and their associated measurements and calculation of abiotic variables are described in detail in (*80*), (*84*) and (*85*).

Prior to the start of any of the treatments in August 2014, one peat soil core up to a depth of 2 m was collected from each plot. Peat samples were dried, ground, and analyzed using a PerkinElmer Spectrum 100 FTIR (Fourier Transform Infrared Spectroscopy) with a Universal ATR accessory. Spectra were collected from 4000 to 650 cm^{-1} at 4 cm^{-1} resolution, with ten scans averaged. After ATR and baseline corrections, peak heights for soil organic matter compounds were normalized and calculated as weight percentages following (*86*). The data and detailed description on the measurement of soil carbohydrate content can be found in (*87*) and (*88*). In August 2019, four years after eCO_2 treatment and five years of whole ecosystem warming treatment, peat soil cores were sampled from +0°C, +4.5°C and +9°C treatments in both ambient (aCO_2) and eCO_2 plots using the same method to measure the soil carbohydrate content.

Porewater samples in each plot were collected in July and August from 2016 to 2022 for CO_2 concentration measurements. Porewater samples were collected from 2.5 cm diameter piezometers installed at depths of 25 to 200 cm in enclosures. Six to twelve piezometers were used per enclosure, with recharging allowed after pumping them dry 12 hours before sampling. Gas diffusion was negligible during this period. Porewater samples for CO_2 analyses were preserved with 10% phosphoric acid and analyzed via headspace analysis using a Finnigan Mat Delta V Isotope Ratio Mass Spectrometer coupled to a gas chromatograph (*89*). The analytical uncertainty for CO_2 concentrations was <5%. The details of the method and data are described in (*90*).

Twenty five 5×5 cm square spots distributed in three community transects within each enclosure were established to estimate the percentage coverage of *Sphagnum* species, including *Sphagnum angustifolium*, *S. fallax* and *S. divinum*. The percentage coverage of these *Sphagnum* species, as well as the percentage of the area that was bare or covered with dead moss (bare dead), were visually estimated each year. The data and details for estimating the percentage coverage of dominant *Sphagnum* species can be found in (*91*) and (*92*). *Sphagnum* productivity was measured using 3.8-cm diameter mesh columns inserted into the peat surface each October. Each column was filled with a known quantity of one of three *Sphagnum* species, with two replicates for each species. After one year, columns were retrieved, samples were oven-dried, and weighed to determine annual productivity. Plot-level *Sphagnum* productivity was estimated by weighting the production of each species by its proportional cover. The data and complete details can be found in (*91*).

Extreme drought identification

We obtained historical water table data at the S1 bog (site of SPRUCE) from (*93*). To identify months of extreme drought in 2021, we calculated the probability density distribution of water table for each month from 1961 to 2021. The extreme drought was defined based on percentile threshold from the distribution (i.e. below 10^{th} percentile) (*94, 95*). July and August in 2021 were considered extremely dry months over the past 61 years (Fig. S1). Moreover, we calculated the probability density distribution of water table for this period over the past six decades. It showed that July to August in 2021 was a period of extreme drought compared to the non-drought years within our study period (2016-2019) (Fig. S13).

Large collar measurement of carbon fluxes

In each plot, a soil collar with the internal diameter of 1.2 m was permanently inserted 10-20 cm into the surface peat to achieve an airtight seal at ground level. A transportable and transparent

enclosure, constructed from a cylindrical aluminum frame (1.3 m diameter by 1.02 m tall) with a transparent polyethylene fitted plastic cover was used to measure community scale net fluxes for CO_2. Open-path CO_2 (LI-7500A; LiCor Inc., Lincoln, NE) infrared sensor was mounted to a carrying device placed on a permanent stainless steel post in the center of each collar. The carbon (C) fluxes were measured monthly during the growing seasons of 2016-2019 and 2021, but not 2020 due to COVID pandemic disruptions.

On each measurement day, multiple measurement series were conducted, typically between 8 am and 3 pm on sunny days, at each plot. Each series included flux measurements under ambient light and subsequently under dark conditions (using an opaque plastic cover). CO_2 fluxes measured under light represent net CO_2 exchange in the collar (negative value indicates C uptake) on that day, and those measured under dark conditions were the collar respiration (positive value indicates C release). In rare cases (< 3%) where the calculated collar gross primary productivity (i.e., collar net CO_2 exchange minus collar respiration) was positive, each measurement series was examined. Because such values were physiologically unrealistic and likely caused by disturbance effects. They were excluded from the final analysis. The details of the method and data are described in (*80, 84, 96*).

Relationships of daily means with the daytime collar measurement of C fluxes

The large-collar measurement was made during daytime (usually between 8 am and 3 pm). To estimate daily means of the C fluxes from the daytime collar measurements, we used high temporal resolution of C fluxes measured in each experimental plot using small chambers during the 2022 and 2023 growing seasons. Note that such high temporal resolution measurements were not available before 2022. In 2022 and 2023, C fluxes were measured using ABB GLA131-GGA CO_2 analyzers, each connected to an Eosense eosMX multiplexer and two eosAC-LT automated clear-top flux chambers (0.5 m diameter), installed on metal collars embedded 15-20 cm into the peat and extending up to 50 cm above the surface. Measurements were taken every 30 minutes in 2022 and every 15 minutes in 2023. Each flux chamber ran a 3-minute sampling period, followed by a 90-second purge, alternating between two chambers in each enclosure. Soil moisture and temperature were measured using Meter Teros 12 sensors installed within 50 cm of each chamber collars. Measurements were averaged over each 3-minute flux measurement, resulting in one value per chamber per closure cycle. Photosynthetically active radiation (PAR) was measured using Apogee SQ-421 quantum sensors placed inside each flux chamber, also averaged over the 3-minute sampling period to match the gas flux interval. Complete details of the method and data are described in (*97*). Since the clear-top automated flux chambers allowed light penetration, the measured CO_2 fluxes represent net CO_2 exchange in the small chamber. Nighttime CO_2 fluxes measured without light (PAR < 0, flux values > 0) were used as a proxy for small chamber respiration.

We used these nighttime CO_2 fluxes and environmental predictors to develop a random forest machine learning model for estimating small chamber respiration every 30 minutes in 2022 and 15 minutes in 2023 over 24 hours. Soil temperature at 30 cm depth, soil volumetric water content at 20 cm depth, warming levels, CO_2 levels and month (account for vegetation dynamics) were used as predictor variables in the random forest model. The data was randomly split into training (80%) and testing (20%) sets with replacement. Hyperparameter tuning was performed on the training set using five-fold cross-validation implemented with the "caret (V7.0.1)" package (*98*). The final model was trained using the optimal mtry = 2, with 1000 trees (ntree=1000), and a minimum node size of 5 (nodesize = 5). The trained model was used to validate against the testing dataset. Model performance was evaluated using mean squared error (MSE) and the coefficient of

determination (R^2). The random forest model showed good predictive performance, with an R^2 of 0.64 and MSE of 2.23 on the training dataset, and an R^2 of 0.60 and MSE of 2.52 on the testing dataset (Fig. S14). The random forest was performed using the "randomForest (V4.7-1.2)" package (*99*).

Based on the observed net CO_2 exchange from high frequency automated chamber and estimated respiration from the random forest model, we calculated average flux values during daytime (8 am to 3 pm) and daily means over the full 24-hour period. To establish robust relationships between daytime C fluxes and their daily mean values, we employed Standardized Major Axis (SMA) regression. Unlike Ordinary Least Squares (OLS) regression, which assumes the independent variable (X) is measured without error and minimizes residuals only in the Y direction, SMA regression accounts for measurement errors in both variables, thereby providing an unbiased, bidirectional conversion between the two variables. This symmetry ensures the relationship is stable and reversible, making SMA the most appropriate approach to characterize the conversion between daytime and daily mean values. This method has been widely used in ecological studies to represent mutual associations where both variables have measurement uncertainties (*100-103*). The SMA regression was performed using the "smatr (V3.4.8)" package (*104*). Analysis revealed good correlations between daytime and daily mean values across these C fluxes (Fig. S15). These relationships were then applied to calculate daily mean fluxes from daytime large collar measurement values.

Estimation of ecosystem carbon fluxes

The large collar chambers cover short-stature plants (e.g., shrubs and forbs but not trees), *Sphagnum* mosses, microbial communities, and roots of all plants, including tree. Thus, C fluxes measured from the large collar chambers do not include tree photosynthesis and tree aboveground autotrophic respiration. We added estimated tree photosynthesis and aboveground autotrophic respiration to the big collar measurements to calculate ecosystem C fluxes, including net ecosystem productivity (NEP), ecosystem respiration (ER), and gross ecosystem productivity (GEP).

Direct measurements of tree photosynthesis and aboveground autotrophic respiration at canopy scale were not available as such measurements are challenging, especially in manipulative experimental plots. At the SPRUCE site, annual tree inventory data from 2016 to 2021 were available, including measurements of diameter at breast height (1.3 m) and tree height (*105*). These data allow for the estimation of annual aboveground biomass through allometric relationships, which can subsequently be used to derive annual aboveground net primary production (ANPP) (*70*) and leaf area index (LAI) for trees (*106*). However, these annual measurements are insufficient to capture C dynamics at finer temporal scales, such as monthly determinations in July and August required in this study. Therefore, we used model estimates of tree photosynthesis and aboveground autotrophic respiration.

We estimated gross primary productivity and aboveground autotrophic respiration of trees for each experimental plot using a data-trained, process-based model (TECO-SPRUCE) (*107, 108*), which was specifically developed for the SPRUCE site. In this model, leaf photosynthesis is calculated using the Farquhar model (*109*), coupled with the Ball-Berry stomatal conductance model (*110*), and then upscaled to canopy photosynthesis through a multilayer process-based model (*111*). Leaf respiration is estimated primarily as a temperature-dependence function. The development and structure of TECO-SPRUCE are comprehensively described in (*108, 112*). To simulate tree C dynamics, the model was driven by treatment-specific hourly meteorological data (*84*), and its key parameters were constrained through a data assimilation method (*113, 114*)

incorporating seventeen observational variables individually collected in each experimental plot at the SPRUCE site. Among these, four aboveground tree-related variables: ANPP, LAI, aboveground tree biomass and leaf-level photosynthetic rates (*115, 116*), were used to optimize model parameters related to tree C processes. After parameter optimization, the estimated values of tree C dynamics closely matched the observations (Fig. S16), providing reliable quantification of hourly tree gross primary productivity and aboveground autotrophic respiration.

The performance of the model was further evaluated using observed daily green chromatic coordinate (GCC) data from PhenoCam (*117*). GCC is a widely used vegetation index from digital images (*118*) and the PhenoCam network provides continuous, high-frequency GCC observations across a variety of ecosystems (*119*), including the SPRUCE site (*120*). GCC effectively captures canopy greenness dynamics and has been shown to closely track seasonal changes in phenology and plant physiological activities (*118, 121*). The strong relationships of modeled tree gross primary productivity and aboveground autotrophic respiration with the observed GCC offer validation of the modeled tree photosynthesis and aboveground autotrophic respiration (Fig. S17).

Finally, the estimated tree gross primary productivity was added to the large collar gross primary productivity to obtain the GEP. The estimated aboveground tree autotrophic respiration was added to the large collar respiration to obtain the ER. NEP was the difference between them. Positive NEP and GEP values indicate C uptake and positive ER values indicate C release. The estimated productivity of trees contributes only a small part to the overall ecosystem productivity. Tree photosynthesis represents 25.0% of the ecosystem GEP, while tree ANPP only accounts for 11.9% of total ecosystem net primary production (*70*). This indicates that the aboveground tree productivity plays a relatively minor role in the ecosystem C dynamics.

Statistical Analysis

To evaluate the impact of extreme drought event on ecosystem C fluxes, we estimated the drought effect as the difference in mean C flux values between the drought period in 2021 and the corresponding period in non-drought years under the same treatment:

$$Drought\ effect = Cflux_{drought} - Cflux_{non-drought}$$

where $Cflux_{drought}$ is the mean C flux during the extreme drought period in 2021, while $Cflux_{non-drought}$ is the mean C flux during the corresponding period in non-drought years (from 2016 to 2019). The effects of extreme drought event on other biotic and abiotic variables were calculated using the same method and their respective observations.

All statistical significance levels were set at $\alpha = 0.05$. Pairwise two-sided Student's *t*-tests were performed to examine the differences in the peat carbohydrate content, porewater CO_2 concentration, as well as drought-induced changes in ecosystem C fluxes and associated biotic and abiotic variables between warming and CO_2 treatments. *P* values were adjusted using the Benjamini-Hochberg false discovery rate (FDR) correction for multiple comparisons, implemented with the "rstatix (V0.7.2)" package (*122*). We used multiple regression analyses to explore the effects of drought-induced changes in biotic/abiotic factors (duration of low-water-table conditions, WT, VPD, temperature, *Sphagnum* biomass, *Sphagnum* coverage, and bare ground or dead moss coverage) on the differences in the drought effect on C fluxes between ambient and eCO_2 conditions. Predictors with a variance inflation factor (VIF) greater than 5 were excluded to reduce redundancy and avoid confounding effects. To visualize the effect of each predictor while controlling for the influence of others in the multiple regression model, predictor effect plots were generated using the "effects (V4.2.2)" package (*123*). These plots show the expected response as a function of one predictor at a time, with all other predictors held at their means. Furthermore, we applied ridge regression to control the collinearity among the drought-

induced changes in these biotic/abiotic covariates, and to evaluate their relative importance on the differential impacts of extreme drought on ecosystem C fluxes under ambient and eCO_2 treatments. The ridge regression was performed using the "ridge (V3.3)" package (*124*). All statistical analyses were conducted in R (version 4.4.3., R Development Core Team).

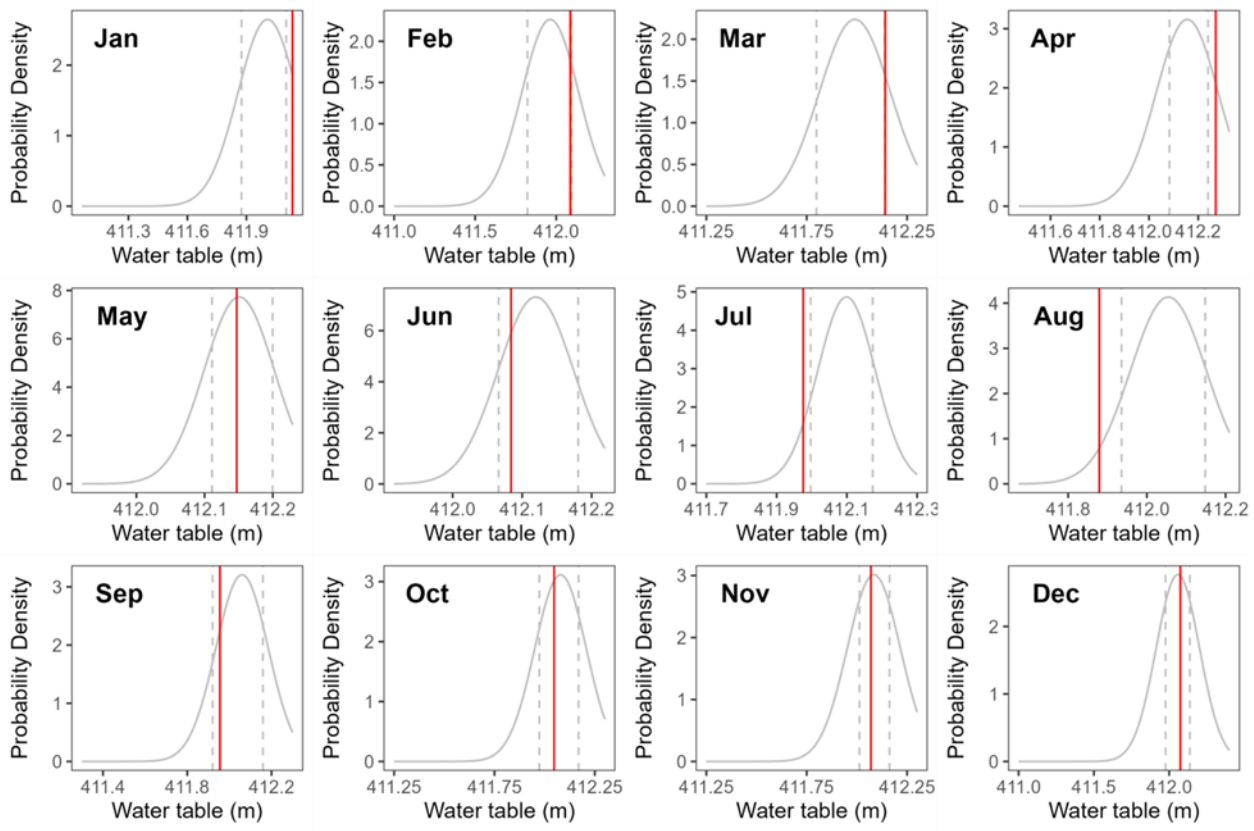

Fig. S1 The probability distribution of water table at the study site for each month from 1961 to 2021. The vertical grey dashed lines represent the 10th and 90th percentile of historical water table, respectively. The red solid lines represent water tables of each month in 2021.

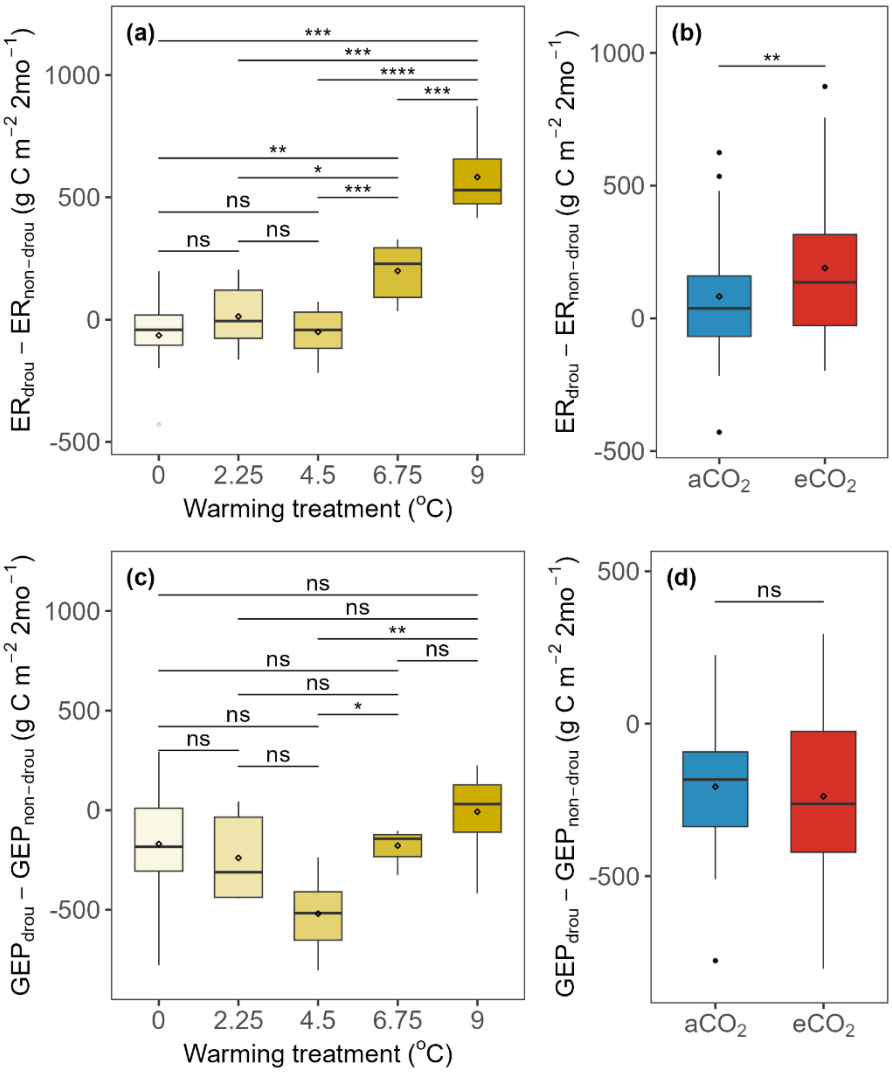

Fig. S2 Effects of extreme drought on (a, b) ecosystem respiration (ER) and (c, d) gross ecosystem productivity (GEP) under different warming and CO_2 treatments. ER_{drou} and $ER_{non\text{-}drou}$ represent ER in the two months in drought year and non-drought years, respectively. The same applies to GEP. The lower and upper boundaries of the boxplots indicate the 25th and 75th quartiles. The center lines represent the median values, the rhombus-shaped points inside the boxes indicate the mean values, and the whiskers represent 1.5 times the interquartile range. The abbreviations "aCO_2" and "eCO_2" refer to ambient and elevated CO_2, respectively. *P* values are adjusted using the Benjamini-Hochberg FDR correction for multiple comparisons. An insignificant difference is indicated by "ns", while *, **, *** and **** indicate significant differences at the 0.05, 0.01, 0.001 and 0.0001 levels, respectively.

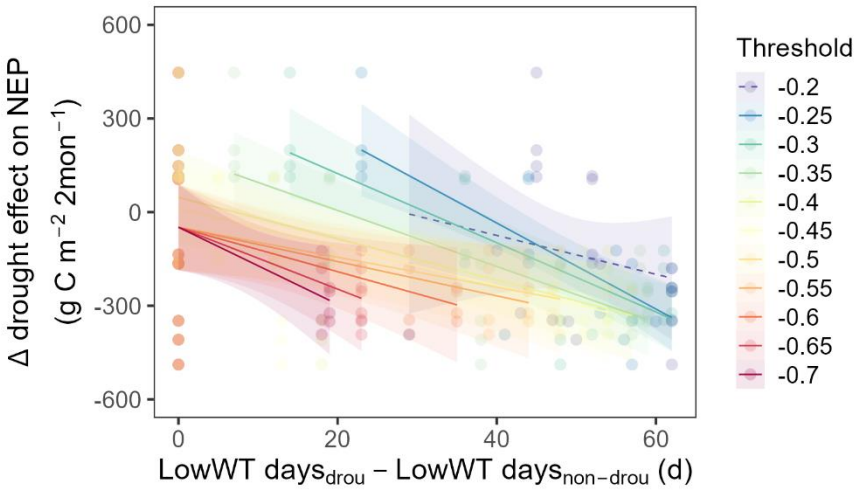

Fig. S3 Relationships between elevated CO_2 (eCO_2)-induced change in the drought effect on net ecosystem productivity (NEP) and drought-induced changes in number of low-water-table (LowWT) days at different water table depth thresholds. Δdrought effect on NEP represents difference in drought effects on NEP between ambient and elevated CO_2 treatments. LowWT $days_{drou}$ and LowWT $days_{non\text{-}drou}$ represent number of days with water table below the threshold in the two months in drought year and non-drought years, respectively. The fitted lines are regressions and the shaded bands are 95% confidence intervals. *P*-values are adjusted using the Benjamini-Hochberg FDR correction. Solid lines show significant relationships and dashed lines indicate insignificant relationships with a significance level set at $\alpha = 0.05$.

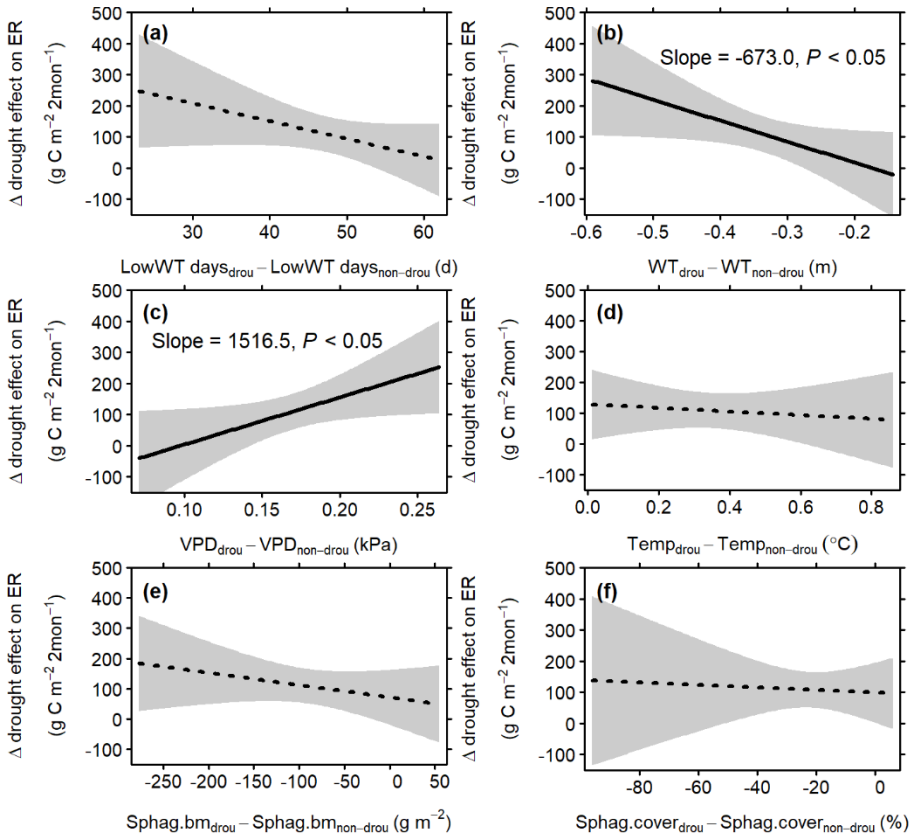

Fig. S4 Difference in drought effects on ecosystem respiration (ER) between ambient and elevated CO_2 treatments as related to various predictors. The difference, denoted by Δdrought effect on ER, depends on drought-induced changes in (a) number of low-water-table (LowWT, below -0.25 m) days, (b) water table depth (WT), (c) vapor pressure deficit (VPD), (d) temperature (Temp), (e) *Sphagnum* biomass (Sphag.bm), and (f) *Sphagnum* coverage (Sphag.cover), respectively. The fitted line shows the estimated effect of each predictor while controlling all other predictors. Solid lines indicate significant effects and dashed lines indicate insignificant effects with a significance level set at $\alpha = 0.05$. The shaded bands are 95% confidence intervals.

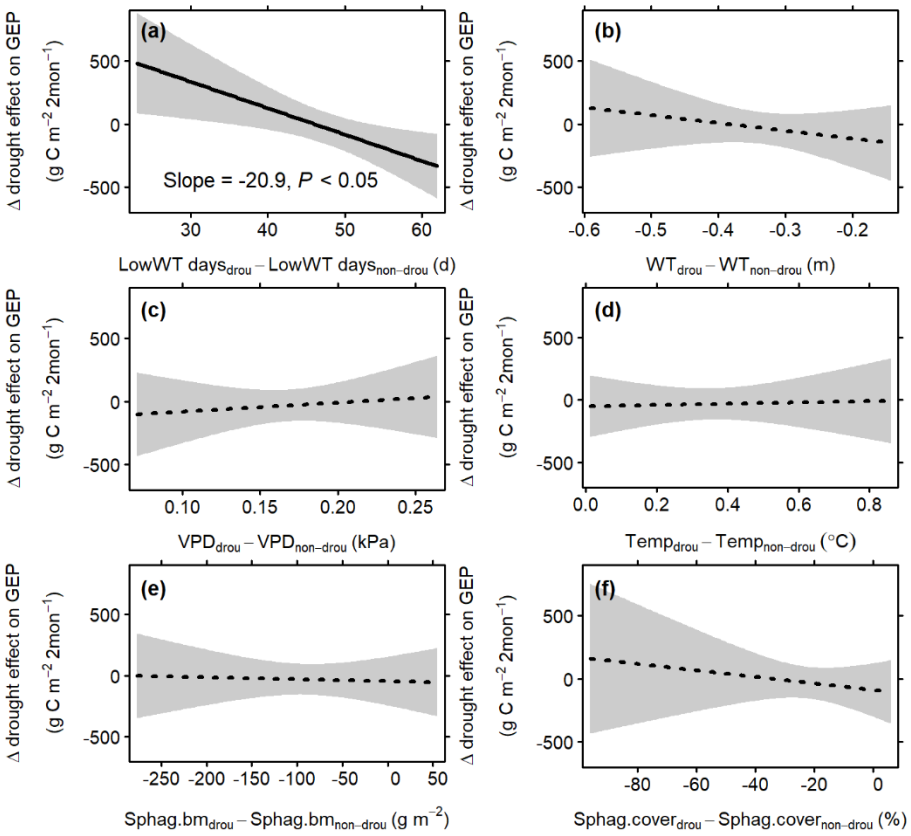

Fig. S5 Difference in drought effects on gross ecosystem productivity (GEP) between ambient and elevated CO_2 treatments as related to various predictors. The difference, denoted by Δdrought effect on GEP, depends on drought-induced changes in (a) number of low-water-table (LowWT, below -0.25 m) days, (b) water table depth (WT), (c) vapor pressure deficit (VPD), (d) temperature (Temp), (e) *Sphagnum* biomass (Sphag.bm), and (f) *Sphagnum* coverage (Sphag.cover), respectively. The fitted line shows the estimated effect of each predictor while controlling all other predictors. Solid lines indicate significant effects and dashed lines indicate insignificant effects with a significance level set at $\alpha = 0.05$. The shaded bands are 95% confidence intervals.

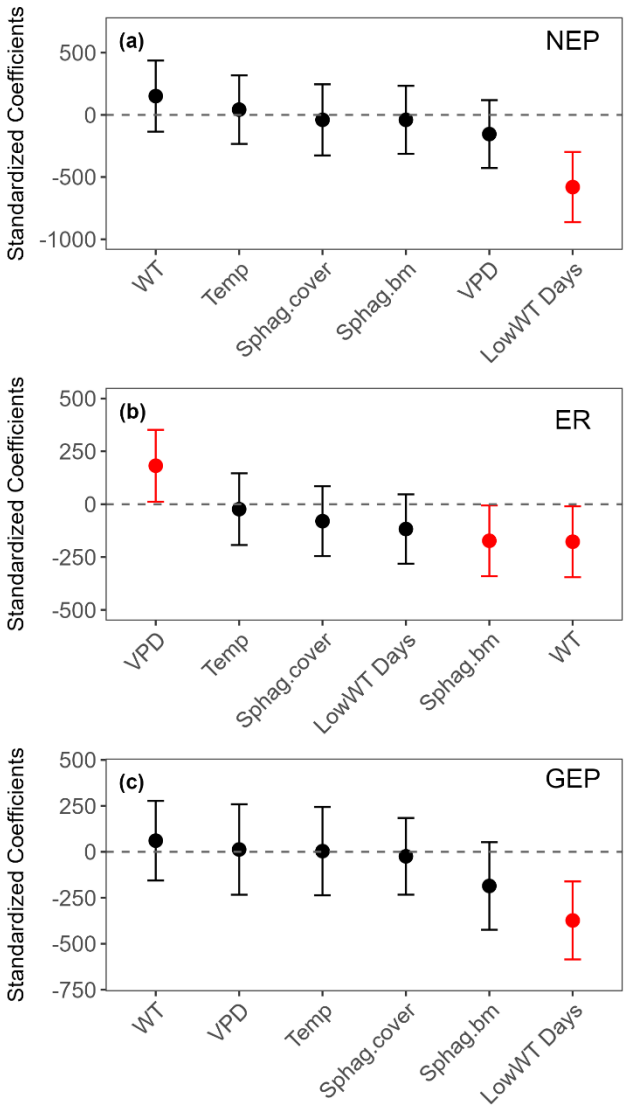

Fig. S6 Contributions of extreme drought-induced changes in biotic and abiotic factors to the differential impacts of extreme drought on ecosystem carbon fluxes under ambient and elevated CO_2 treatments. (a) net ecosystem productivity (NEP), (b) ecosystem respiration (ER) and (c) gross ecosystem productivity (GEP). LowWT Days: number of low-water-table (below -0.25 m) days; WT: water table depth; VPD: vapor pressure deficit; Temp: temperature; Sphag.bm: *Sphagnum* biomass; Sphag.cover: *Sphagnum* coverage. Circles indicate the scaled coefficients of each predictor from the ridge regression, representing their relative importance. Error bars represent 95% confidence intervals. Red indicates significant factors while black for insignificant factors.

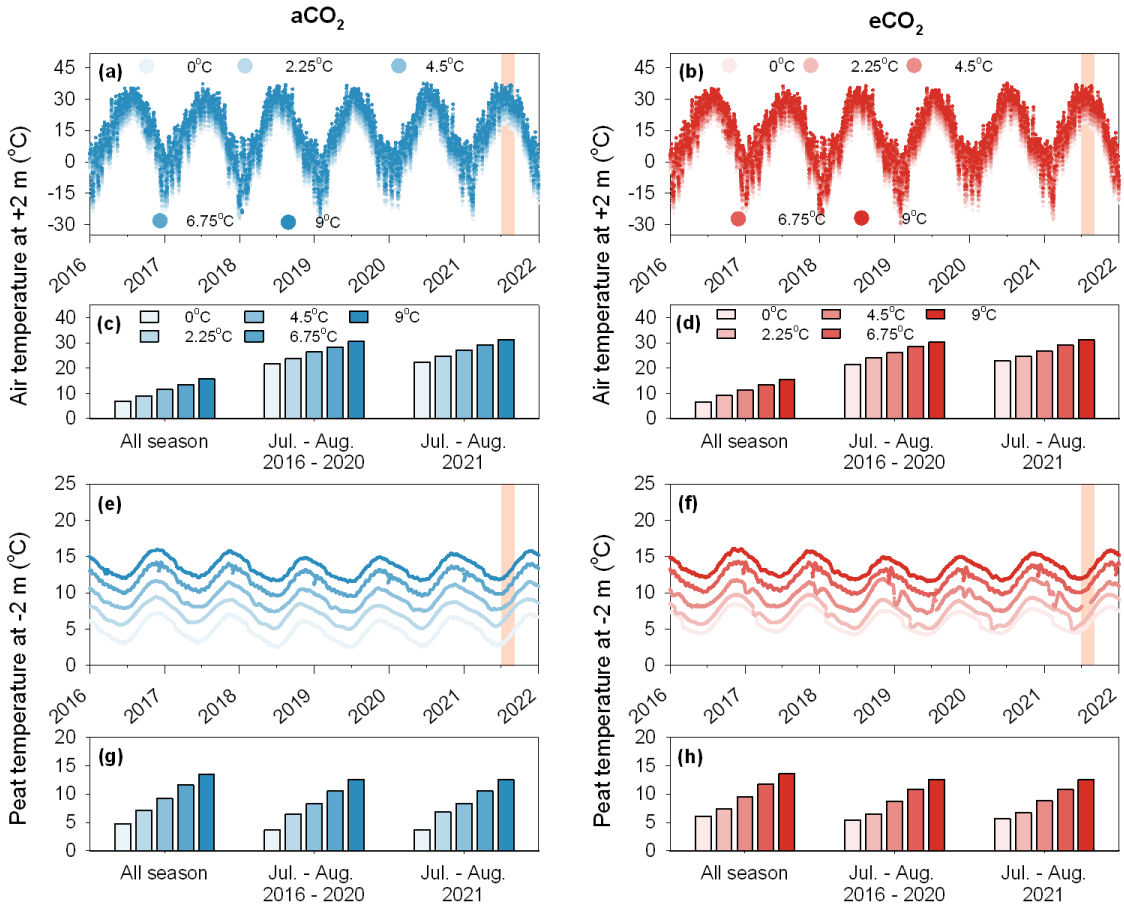

Fig. S7 Patterns of air (a,b) and peat soil (e,f) temperature from 2016 to 2021 under five warming and two CO_2 treatments. Seasonal means of air (c,d) and peat soil (g,h) temperature across years and during drought periods in non-drought (2016-2020) and drought (2021) years under five warming and two CO_2 treatments. Time series data are shown at a daily resolution. Shaded areas indicate the extreme drought period. The abbreviations "aCO_2" and "eCO_2" refer to ambient and elevated CO_2, respectively.

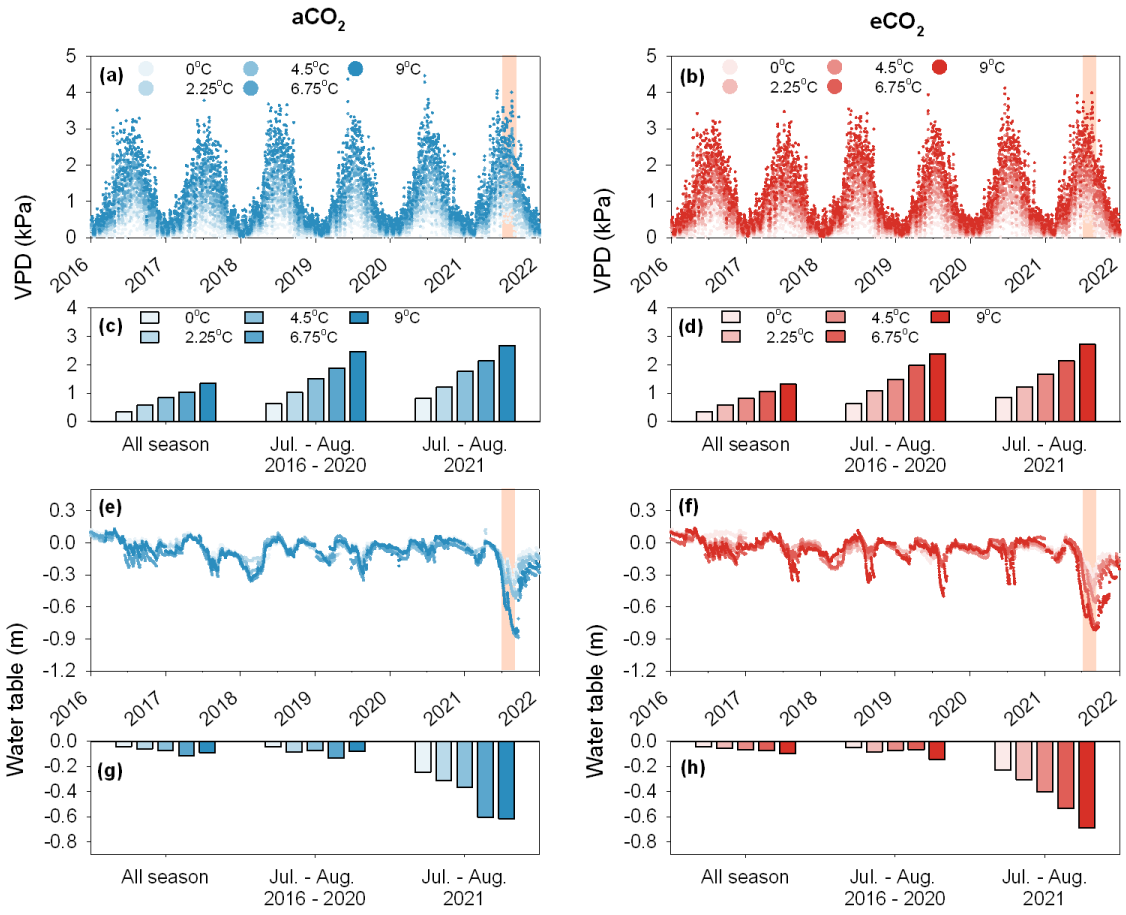

Fig. S8 Patterns of vapor pressure deficit (VPD) (a,b) and water table depth (WT) fluctuations (e,f) from 2016 to 2021 under five warming and two CO_2 treatments. Seasonal means of VPD (c,d) and WT (g,h) across years and during drought periods in non-drought (2016-2020) and drought (2021) years under different warming and CO_2 treatments. Time series data are shown at a daily resolution. Shaded areas indicate the extreme drought period. The abbreviations "aCO_2" and "eCO_2" refer to ambient and elevated CO_2, respectively.

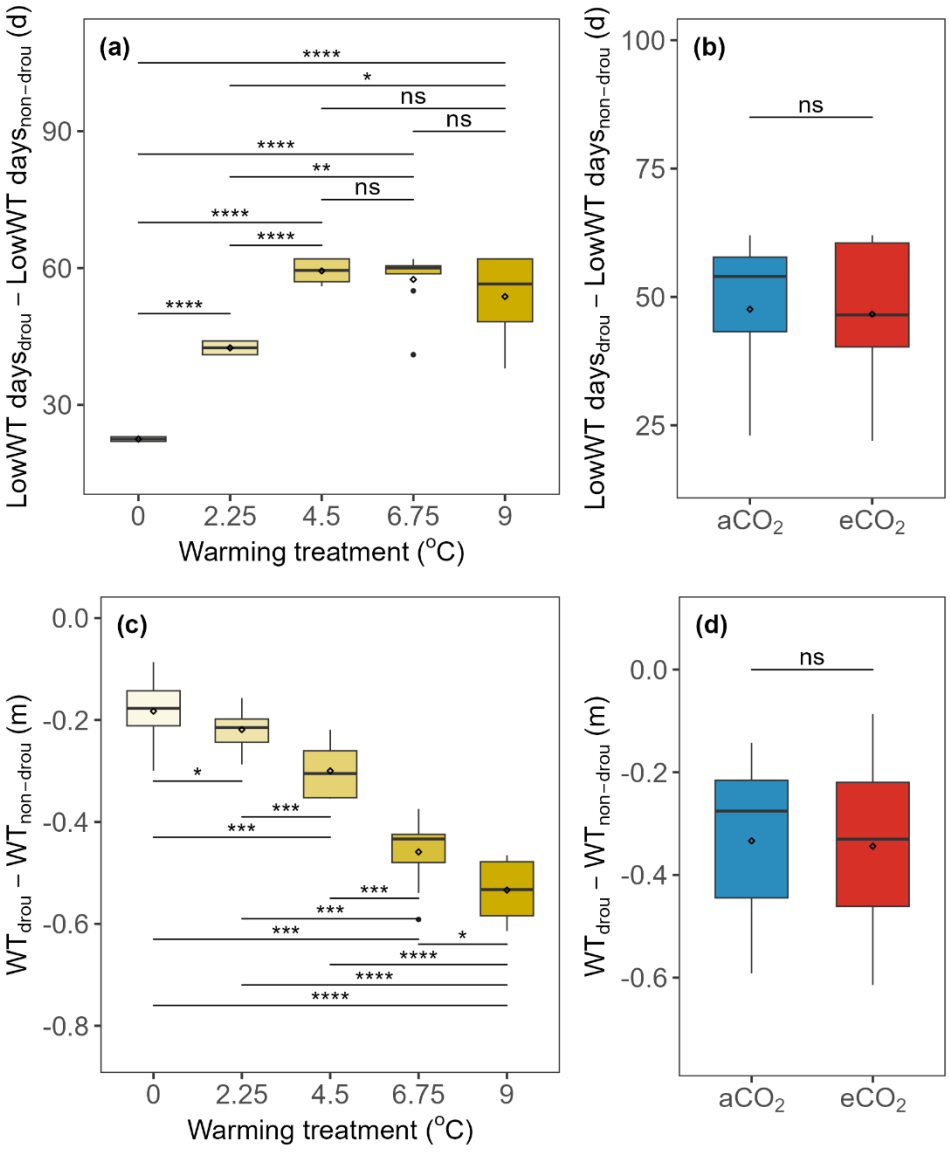

Fig. S9 Effects of extreme drought on (a, b) number of low-water-table (LowWT, below -0.25 m) days and (c, d) water table depth (WT) under five warming and two CO_2 treatments. LowWT days$_{drou}$ and LowWT days$_{non-drou}$ represent number of days with WT below -0.25 m in the two months in drought year and non-drought years, respectively. The same applies to WT. The lower and upper boundaries of the boxplots indicate the 25th and 75th quartiles. The center lines represent the median values, the rhombus-shaped points inside the boxes indicate the mean values, and the whiskers represent 1.5 times the interquartile range. The abbreviations "aCO_2" and "eCO_2" refer to ambient and elevated CO_2, respectively. *P* values are adjusted using the Benjamini-Hochberg FDR correction for multiple comparisons. An insignificant difference is indicated by "ns", while *, **, *** and **** indicate significant differences at the 0.05, 0.01, 0.001 and 0.0001 levels, respectively.

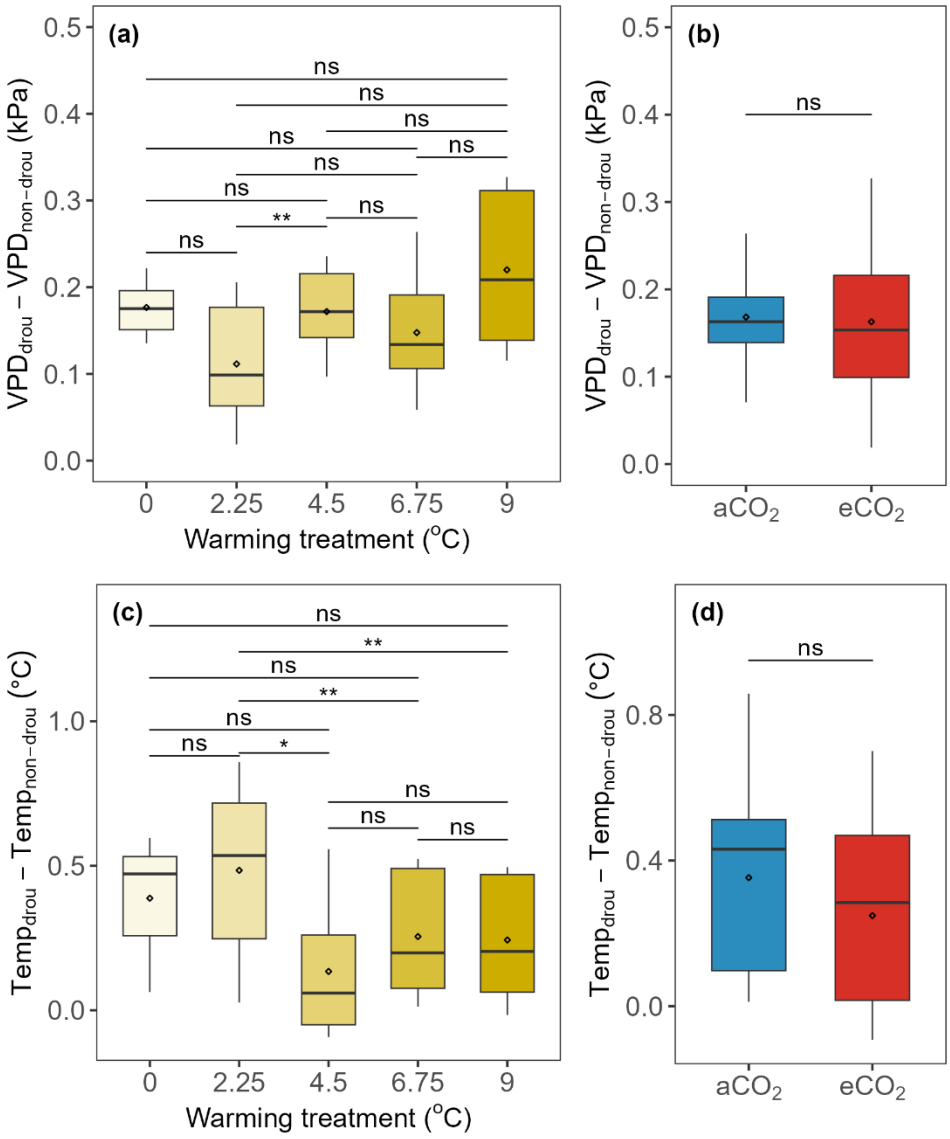

Fig. S10 Effects of extreme drought on (a, b) vapor pressure deficit (VPD) and (c, d) temperature (Temp) under five warming and two CO_2 treatments. VPD_{drou} and $VPD_{non\text{-}drou}$ represent VPD in the two months in drought year and non-drought years, respectively. The same applies to Temp. The lower and upper boundaries of the boxplots indicate the 25th and 75th quartiles. The center lines represent the median values, the rhombus-shaped points inside the boxes indicate the mean values, and the whiskers represent 1.5 times the interquartile range. The abbreviations "aCO_2" and "eCO_2" refer to ambient and elevated CO_2, respectively. *P* values are adjusted using the Benjamini-Hochberg FDR correction for multiple comparisons. An insignificant difference is indicated by "ns", while * and ** indicate significant differences at the 0.05 and 0.01 levels, respectively.

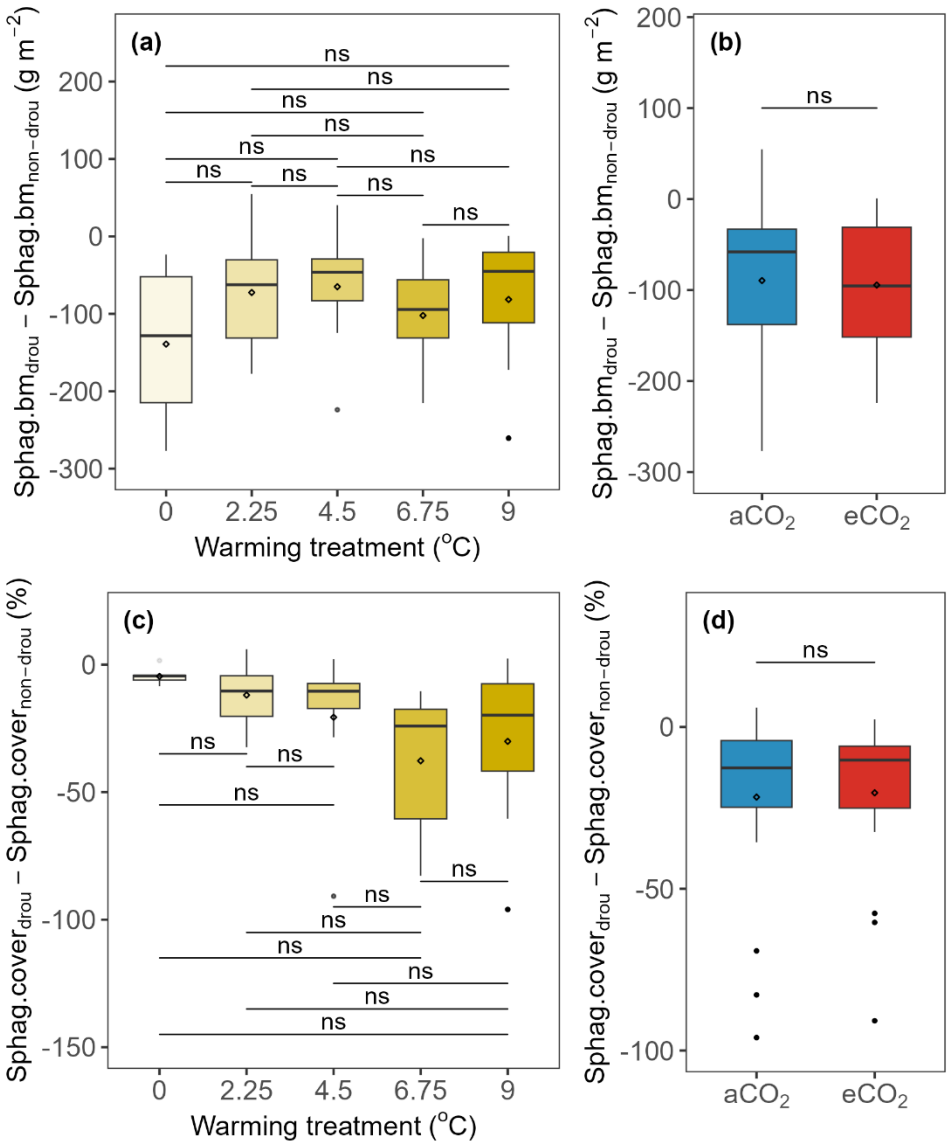

Fig. S11 Effects of extreme drought on (a, b) *Sphagnum* biomass (Sphag.bm) and (c, d) *Sphagnum* coverage (Sphag.cover) under five warming and two CO_2 treatments. Sphag.bm$_{drou}$ and Sphag.bm$_{non\text{-}drou}$ represent *Sphagnum* biomass in drought year and non-drought years, respectively. The same applies to Sphag.cover. The lower and upper boundaries of the boxplots indicate the 25th and 75th quartiles. The center lines represent the median values, the rhombus-shaped points inside the boxes indicate the mean values, and the whiskers represent 1.5 times the interquartile range. The abbreviations "aCO_2" and "eCO_2" refer to ambient and elevated CO_2, respectively. *P* values are adjusted using the Benjamini-Hochberg FDR correction for multiple comparisons. An insignificant difference is indicated by "ns", while * indicates significant differences at the 0.05 level, respectively.

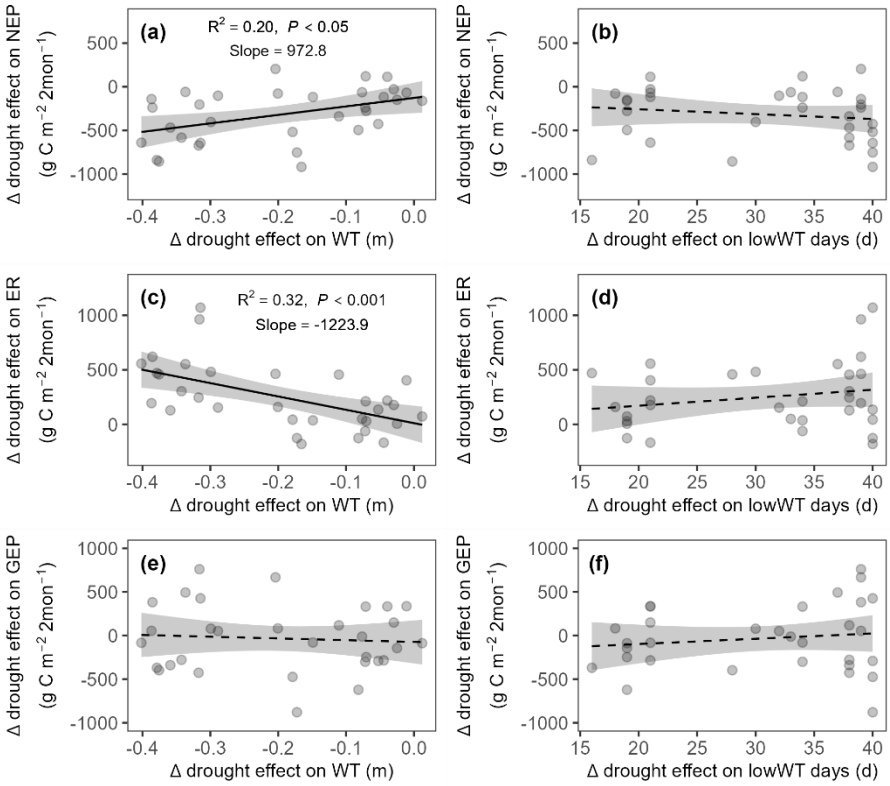

Fig. S12 Relationships between warming-induced changes in the drought effects on water table depth (WT), number of low-water-table (LowWT, below -0.25 m) days and warming-induced changes in the drought effect on (a, b) net ecosystem productivity (NEP), (c, d) ecosystem respiration (ER), and (e, f) gross ecosystem productivity (GEP), respectively. The fitted lines are regressions and the shaded bands are 95% confidence intervals. Solid lines show significant relationships and dashed lines indicate insignificant relationships with a significance level set at $\alpha = 0.05$.

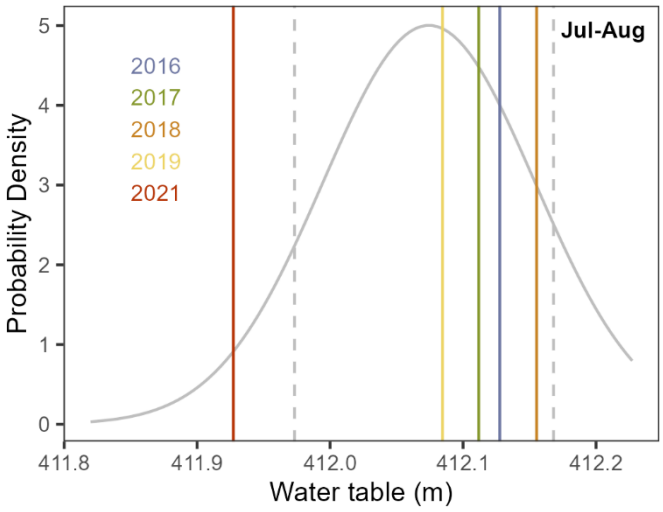

Fig. S13 Probability distribution of water table at the study site during July to August from 1961 to 2021. The vertical grey dashed lines represent the 10^{th} and 90^{th} percentiles of historical water tables, respectively. The colored vertical solid lines represent water table during July-August in each year during the study period.

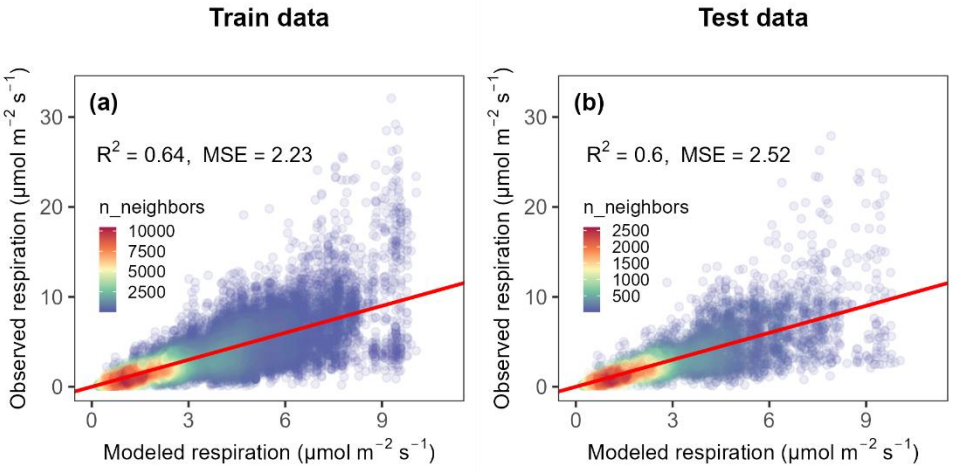

Fig. S14 Relationship between observed and modeled small-chamber respiration for the (a) training and (b) testing datasets based on the random forest model. Observed CR values were obtained from nighttime measurements using automated flux chambers, and modeled CR values were predicted by the random forest model. The red line indicates the 1:1 line.

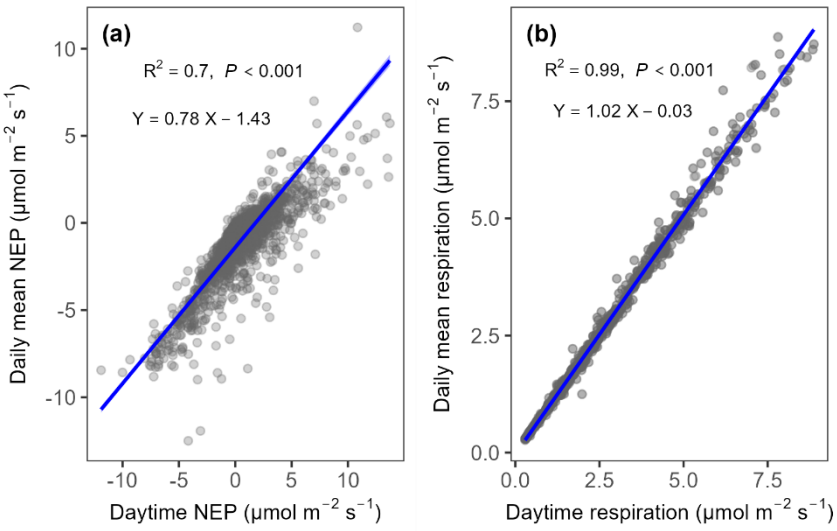

Fig. S15 Relationships between daytime (08:00 – 15:00) and daily mean carbon fluxes for (a) net ecosystem productivity (NEP), (b) respiration in the small chamber.

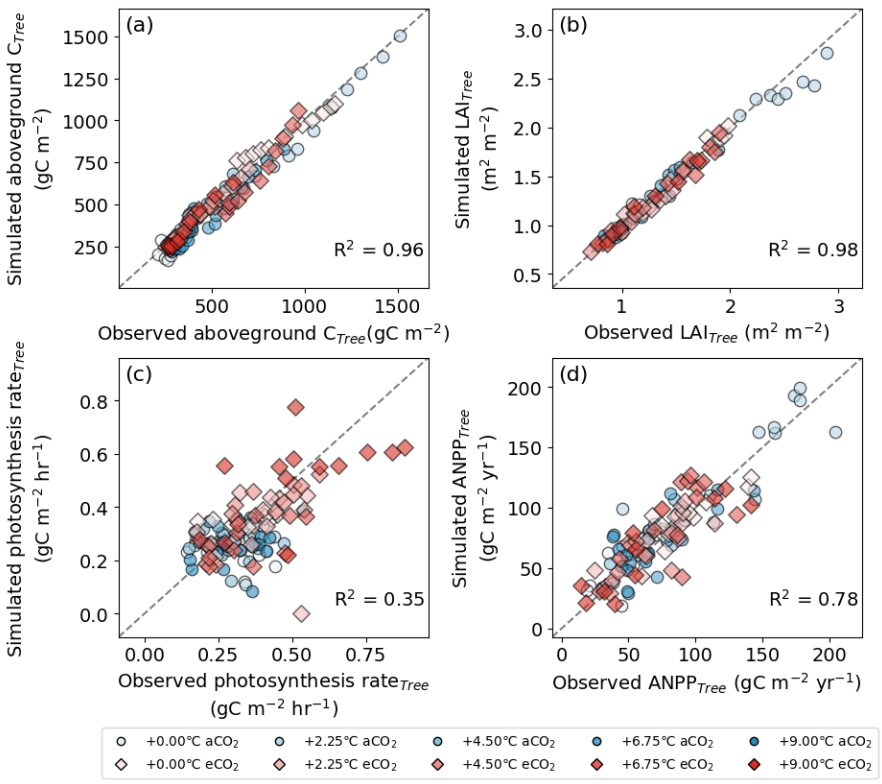

Fig. S16 Relationships between observed and modeled variables for (a) aboveground tree C, (b) leaf area index (LAI), (c) tree photosynthesis rate and (d) aboveground net primary production ($ANPP_{Tree}$).

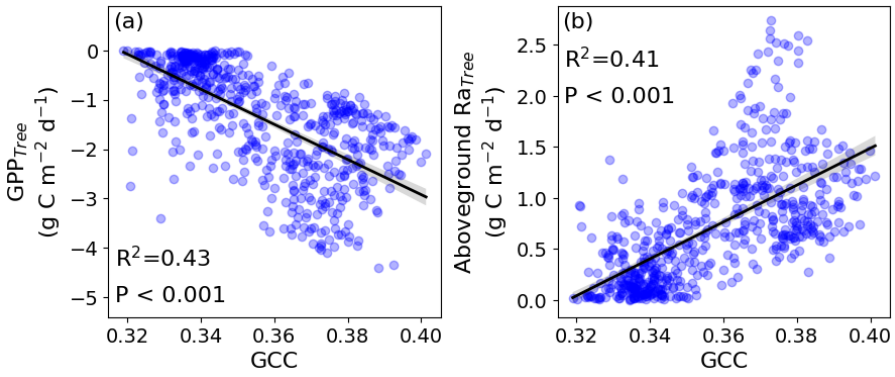

Fig. S17 Relationships between mean monthly green chromatic coordinate (GCC) and mean monthly values of (a) tree gross primary productivity (GPP_{Tree}), and (b) tree aboveground autotrophic respiration (Ra_{Tree}).

Table S1 Results of multiple regression analysis assessing the effects of drought-induced changes in biotic and abiotic factors on the difference in drought effects on net ecosystem productivity (NEP) between ambient and elevated CO_2 treatments. The table reports estimated coefficients, standard errors, t-values, and *P*-values for each predictor. LowWT days: number of low-water-table (below -0.25 m) days; WT: water table depth; VPD: vapor pressure deficit; Temp: temperature; Sphag.bm: *Sphagnum* biomass; Sphag.cover: *Sphagnum* coverage.

	Coefficient	Std. Error	t	*P*	R^2
LowWT days	-15.23	4.78	-3.18	***P* < 0.01**	0.67
WT	56.65	439.45	0.13	*P* = 0.90	
VPD	-797.05	978.34	-0.82	*P* = 0.43	
Temp	109.48	193.76	0.57	*P* = 0.58	
Sphag.bm	0.25	0.53	0.47	*P* = 0.65	
Sphag.cover	-2.18	2.43	-0.90	*P* = 0.39	
Intercept	674.77	212.51	3.18	*P* < 0.01	

Table S2 Results of multiple regression analysis assessing the effects of drought-induced changes in biotic and abiotic factors on the difference in drought effects on ecosystem respiration (ER) between ambient and elevated CO_2 treatments. The table reports estimated coefficients, standard errors, t-values, and *P*-values for each predictor. LowWT days: number of low-water-table (below -0.25 m) days; WT: water table depth; VPD: vapor pressure deficit; Temp: temperature; Sphag.bm: *Sphagnum* biomass; Sphag.cover: *Sphagnum* coverage.

	Coefficient	Std. Error	t	*P*	R^2
LowWT days	-5.68	3.26	-1.75	*P* = 0.10	0.58
WT	-673.05	299.04	-2.25	***P* < 0.05**	
VPD	1516.55	665.75	2.28	***P* < 0.05**	
Temp	-58.95	131.85	-0.45	*P* = 0.66	
Sphag.bm	-0.41	0.36	-1.12	*P* = 0.28	
Sphag.cover	-0.40	1.65	-0.24	*P* = 0.81	
Intercept	-125.74	144.61	-0.87	*P* = 0.40	

Table S3 Results of multiple regression analysis assessing the effects of drought-induced changes in biotic and abiotic factors on the difference in drought effects on gross ecosystem productivity (GEP) between ambient and elevated CO_2 treatments. The table reports estimated coefficients, standard errors, t-values, and *P*-values for each predictor. LowWT days: number of low-water-table (below -0.25 m) days; WT: water table depth; VPD: vapor pressure deficit; Temp: temperature; Sphag.bm: *Sphagnum* biomass; Sphag.cover: *Sphagnum* coverage.

	Coefficient	Std. Error	t	*P*	R^2
LowWT days	-20.91	7.12	-2.94	***P* < 0.05**	0.53
WT	-616.40	653.73	-0.94	*P* = 0.36	
VPD	719.50	1455.40	0.49	*P* = 0.63	
Temp	50.53	288.24	0.18	*P* = 0.86	
Sphag.bm	-0.15	0.80	-0.19	*P* = 0.85	
Sphag.cover	-2.58	3.61	-0.71	*P* = 0.49	
Intercept	549.03	316.14	1.74	*P* = 0.11	

References and Notes

1. IPCC, *Climate Change 2021: The Physical Science Basis. Contribution of Working Group I to the Sixth Assessment Report of the Intergovernmental Panel on Climate Change*, V. Masson-Delmotte, P. Zhai, A. Pirani, S. L. Connors, C. Péan, S. Berger, N. Caud, Y. Chen, L. Goldfarb, M. I. Gomis, M. Huang, K. Leitzell, E. Lonnoy, J. B. R. Matthews, T. K. Maycock, T. Waterfield, O. Yelekçi, R. Yu, B. Zhou, Eds. (Cambridge Univ. Press, 2021).

2. B. D. Stocker, J. Zscheischler, T. F. Keenan, I. C. Prentice, S. I. Seneviratne, J. Peñuelas, Drought impacts on terrestrial primary production underestimated by satellite monitoring. *Nat. Geosci.* **12**, 264–270 (2019).

3. A. Bastos, P. Ciais, P. Friedlingstein, S. Sitch, J. Pongratz, L. Fan, J. P. Wigneron, U. Weber, M. Reichstein, Z. Fu, P. Anthoni, A. Arneth, V. Haverd, A. K. Jain, E. Joetzjer, J. Knauer, S. Lienert, T. Loughran, P. C. McGuire, H. Tian, N. Viovy, S. Zaehle, Direct and seasonal legacy effects of the 2018 heat wave and drought on European ecosystem productivity. *Sci. Adv.* **6**, eaba2724 (2020).

4. E. Martínez-García, M. B. Nilsson, H. Laudon, T. Lundmark, J. E. S. Fransson, J. Wallerman, M. Peichl, Drought response of the boreal forest carbon sink is driven by understorey-tree composition. *Nat. Geosci.* **17**, 197–204 (2024).

5. A. C. Bennett, T. Rodrigues de Sousa, A. Monteagudo-Mendoza, A. Esquivel-Muelbert, P. S. Morandi, F. Coelho de Souza, W. Castro, L. F. Duque, G. Flores Llampazo, R. Manoel dos Santos, E. Ramos, E. Vilanova Torre, E. Alvarez-Davila, T. R. Baker, F. R. C. Costa, S. L. Lewis, B. S. Marimon, J. Schietti, B. Burban, E. Berenguer, A. Araujo-Murakami, Z. Restrepo Correa, W. Lopez, F. Delgado Santana, L. J. Viscarra, F. Elias, R. Vasquez Martinez, B. H. Marimon-Junior, D. Galbraith, M. J. P. Sullivan, T. Emilio, N. C. C. S. Prestes, J. Barlow, N. C. Alencar Fagundes, E. Almeida de Oliveira, P. Alvarez Loayza, L. F. Alves, S. Aparecida Vieira, V. Andrade Maia, L. E. O. C. Aragão, E. J. M. M. Arets, L. Arroyo, O. Bánki, C. Baraloto, P. Barbosa Camargo, J. Barroso, W. Bento da Silva, D. Bonal, A. Borges Miranda Santos, R. J. W. Brienen, F. Brown, C. V. Castilho, S. Cerruto Ribeiro, V. Chama Moscoso, E. Chavez, J. A. Comiskey, F. Cornejo Valverde, N. Dávila Cardozo, N. de Aguiar-Campos, L. de Oliveira Melo, J. del Aguila Pasquel, G. Derroire, M. Disney, M. do Socorro, A. Dourdain, T. R. Feldpausch, J. Ferreira, V. Forni Martins, T. Gardner, E. Gloor, G. Gutierrez Sibauty, R. Guillen, E. Hase, B. Hérault, E. N. Honorio Coronado, W. Huaraca Huasco, J. P. Janovec, E. Jimenez-Rojas, C. Joly, M. Kalamandeen, T. J. Killeen, C. Lais Farrapo, A. Levesley, L. Lizon Romano, G. Lopez Gonzalez, F. A. Maës dos Santos, W. E. Magnusson, Y. Malhi, S. Matias de Almeida Reis, K. Melgaço, O. A. Melo Cruz, I. Mendoza Polo, T. Montañez, J. D. Morel, M. P. Núñez Vargas, R. Oliveira de Araújo, N. C. Pallqui Camacho, A. Parada Gutierrez, T. Pennington, G. C. Pickavance, J. Pipoly, N. C. A. Pitman, C. Quesada, F. Ramirez Arevalo, H. Ramírez-Angulo, R. Flora Ramos, J. E. Richardson, C. Rodrigo de Souza, A. Roopsind, G. Schwartz, R. C. Silva, J. Silva Espejo, M. Silveira, J. Singh, Y. Soto Shareva, M. Steininger, J. Stropp, J. Talbot, H. ter Steege, J. Terborgh, R. Thomas, L. Valenzuela Gamarra, G. van der Heijden, P. van der Hout, R. Zagt, O. L. Phillips, Sensitivity of South American tropical forests to an extreme climate anomaly. *Nat. Clim. Chang.* **13**, 967–974 (2023).

6. D. Gampe, J. Zscheischler, M. Reichstein, M. O'Sullivan, W. K. Smith, S. Sitch, W. Buermann, Increasing impact of warm droughts on northern ecosystem productivity over recent decades. *Nat. Clim. Chang.* **11**, 772–779 (2021).

7. Q. Quan, D. Tian, Y. Luo, F. Zhang, T. W. Crowther, K. Zhu, H. Y. H. Chen, Q. Zhou, S. Niu, Water scaling of ecosystem carbon cycle feedback to climate warming. *Sci. Adv.* **5**, eaav1131 (2019).

8. P. Ciais, M. Reichstein, N. Viovy, A. Granier, J. Ogée, V. Allard, M. Aubinet, N. Buchmann, C. Bernhofer, A. Carrara, F. Chevallier, N. De Noblet, A. D. Friend, P. Friedlingstein, T. Grünwald, B. Heinesch, P. Keronen, A. Knohl, G. Krinner, D. Loustau, G. Manca, G. Matteucci, F. Miglietta, J. M. Ourcival, D. Papale, K. Pilegaard, S. Rambal, G. Seufert, J. F. Soussana, M. J. Sanz, E. D. Schulze, T. Vesala, R. Valentini, Europe-wide reduction in primary productivity caused by the heat and drought in 2003. *Nature* **437**, 529–533 (2005).

9. S. Wolf, T. F. Keenan, J. B. Fisher, D. D. Baldocchi, A. R. Desai, A. D. Richardson, R. L. Scott, B. E. Law, M. E. Litvak, N. A. Brunsell, W. Peters, I. T. van der Laan-Luijkx, Warm spring reduced carbon cycle impact of the 2012 US summer drought. *Proc. Natl. Acad. Sci. U.S.A.* **113**, 5880–5885 (2016).

10. C. Werner, L. K. Meredith, S. N. Ladd, J. Ingrisch, A. Kübert, J. van Haren, M. Bahn, K. Bailey, I. Bamberger, M. Beyer, D. Blomdahl, J. Byron, E. Daber, J. Deleeuw, M. A. Dippold, J. Fudyma, J. Gil-Loaiza, L. K. Honeker, J. Hu, J. Huang, T. Klüpfel, J. Krechmer, J. Kreuzwieser, K. Kühnhammer, M. M. Lehmann, K. Meeran, P. K. Misztal, W.-R. Ng, E. Pfannerstill, G. Pugliese, G. Purser, J. Roscioli, L. Shi, M. Tfaily, J. Williams, Ecosystem fluxes during drought and recovery in an experimental forest. *Science* **374**, 1514–1518 (2021).

11. Y. Yang, S. S. Saatchi, L. Xu, Y. Yu, S. Choi, N. Phillips, R. Kennedy, M. Keller, Y. Knyazikhin, R. B. Myneni, Post-drought decline of the Amazon carbon sink. *Nat. Commun.* **9**, 3172 (2018).

12. J. Liu, D. Baker, S. Basu, K. Bowman, B. Byrne, F. Chevallier, W. He, F. Jiang, M. S. Johnson, T. L. Kubar, X. Li, Z. Liu, S. M. Miller, S. Philip, J. Xiao, J. Yun, N. Zeng, The reduced net carbon uptake over Northern Hemisphere land causes the close-to-normal CO_2 growth rate in 2021 La Niña. *Sci. Adv.* **10**, eadl2201 (2024).

13. O. L. Phillips, L. E. O. C. Aragão, S. L. Lewis, J. B. Fisher, J. Lloyd, G. López-González, Y. Malhi, A. Monteagudo, J. Peacock, C. A. Quesada, G. van der Heijden, S. Almeida, I. Amaral, L. Arroyo, G. Aymard, T. R. Baker, O. Bánki, L. Blanc, D. Bonal, P. Brando, J. Chave, Á. C. A. de Oliveira, N. D. Cardozo, C. I. Czimczik, T. R. Feldpausch, M. A. Freitas, E. Gloor, N. Higuchi, E. Jiménez, G. Lloyd, P. Meir, C. Mendoza, A. Morel, D. A. Neill, D. Nepstad, S. Patiño, M. C. Peñuela, A. Prieto, F. Ramírez, M. Schwarz, J. Silva, M. Silveira, A. S. Thomas, H. T. Steege, J. Stropp, R. Vásquez, P. Zelazowski, E. Alvarez Dávila, S. Andelman, A. Andrade, K.-J. Chao, T. Erwin, A. Di Fiore, E. Honorio C, H. Keeling, T. J. Killeen, W. F. Laurance, A. Peña Cruz, N. C. A. Pitman, P. Núñez Vargas, H. Ramírez-Angulo, A. Rudas, R. Salamão, N. Silva, J. Terborgh, A. Torres-Lezama, Drought sensitivity of the Amazon rainforest. *Science* **323**, 1344–1347 (2009).

14. M. Reichstein, M. Bahn, P. Ciais, D. Frank, M. D. Mahecha, S. I. Seneviratne, J. Zscheischler, C. Beer, N. Buchmann, D. C. Frank, D. Papale, A. Rammig, P. Smith, K. Thonicke, M. van der Velde, S. Vicca, A. Walz, M. Wattenbach, Climate extremes and the carbon cycle. *Nature* **500**, 287–295 (2013).

15. D. Frank, M. Reichstein, M. Bahn, K. Thonicke, D. Frank, M. D. Mahecha, P. Smith, M. van der Velde, S. Vicca, F. Babst, C. Beer, N. Buchmann, J. G. Canadell, P. Ciais, W. Cramer, A. Ibrom, F. Miglietta, B. Poulter, A. Rammig, S. I. Seneviratne, A. Walz, M. Wattenbach, M. A. Zavala, J. Zscheischler, Effects of climate extremes on the terrestrial carbon cycle: Concepts, processes and potential future impacts. *Glob. Chang. Biol.* **21**, 2861–2880 (2015).

16. S. Sippel, M. Reichstein, X. Ma, M. D. Mahecha, H. Lange, M. Flach, D. Frank, Drought, Heat, and the Carbon Cycle: A Review. *Curr. Clim. Change Rep.* **4**, 266–286 (2018).

17. J. Song, S. Wan, S. Piao, A. K. Knapp, A. T. Classen, S. Vicca, P. Ciais, M. J. Hovenden, S. Leuzinger, C. Beier, P. Kardol, J. Xia, Q. Liu, J. Ru, Z. Zhou, Y. Luo, D. Guo, J. Adam Langley, J. Zscheischler, J. S. Dukes, J. Tang, J. Chen, K. S. Hofmockel, L. M. Kueppers, L. Rustad, L. Liu, M. D. Smith, P. H. Templer, R. Quinn Thomas, R. J. Norby, R. P. Phillips, S. Niu, S. Fatichi, Y. Wang, P. Shao, H. Han, D. Wang, L. Lei, J. Wang, X. Li, Q. Zhang, X. Li, F. Su, B. Liu, F. Yang, G. Ma, G. Li, Y. Liu, Y. Liu, Z. Yang, K. Zhang, Y. Miao, M. Hu, C. Yan, A. Zhang, M. Zhong, Y. Hui, Y. Li, M. Zheng, A meta-analysis of 1,119 manipulative experiments on terrestrial carbon-cycling responses to global change. *Nat. Ecol. Evol.* **3**, 1309–1320 (2019).

18. C. G. Jung, X. Xu, S. Niu, J. Liang, X. Chen, Z. Shi, L. Jiang, Y. Luo, Experimental warming amplified opposite impacts of drought vs. wet extremes on ecosystem carbon cycle in a tallgrass prairie. *Agric. For. Meteorol.* **276-277**, 107635 (2019).

19. S. Salimi, M. Berggren, M. Scholz, Response of the peatland carbon dioxide sink function to future climate change scenarios and water level management. *Glob. Chang. Biol.* **27**, 5154–5168 (2021).

20. K. E. Mueller, D. M. Blumenthal, E. Pendall, Y. Carrillo, F. A. Dijkstra, D. G. Williams, R. F. Follett, J. A. Morgan, Impacts of warming and elevated CO2 on a semi-arid grassland are non-additive, shift with precipitation, and reverse over time. *Ecol. Lett.* **19**, 956–966 (2016).

21. J. A. Morgan, D. R. LeCain, E. Pendall, D. M. Blumenthal, B. A. Kimball, Y. Carrillo, D. G. Williams, J. Heisler-White, F. A. Dijkstra, M. West, C4 grasses prosper as carbon dioxide eliminates desiccation in warmed semi-arid grassland. *Nature* **476**, 202–205 (2011).

22. P. M. A. Fransson, A. F. S. Taylor, R. D. Finlay, A. B. Cousins, B. A. Kimball, P. J. Pinter Jr., R. L. LaMorte, J. Triggs, M. J. Ottman, S. W. Leavitt, A. D. Matthias, D. G. Williams, A. N. Webber, Elevated atmospheric CO_2 alters root symbiont community structure in forest trees. *New Phytol.* **152**, 431–442 (2001).

23. J. Radolinski, M. Vremec, H. Wachter, S. Birk, N. Brüggemann, M. Herndl, A. Kahmen, D. B. Nelson, A. Kübert, A. Schaumberger, C. Stumpp, M. Tissink, C. Werner, M. Bahn, Drought in a warmer, CO_2-rich climate restricts grassland water use and soil water mixing. *Science* **387**, 290–296 (2025).

24. S. Leuzinger, C. Körner, Water savings in mature deciduous forest trees under elevated CO2. *Glob. Change Biol.* **13**, 2498–2508 (2007).

25. Z. Wang, C. Wang, S. Liu, Elevated CO2 alleviates adverse effects of drought on plant water relations and photosynthesis: A global meta-analysis. *J. Ecol.* **110**, 2836–2849 (2022).

26. J. Roy, C. Picon-Cochard, A. Augusti, M.-L. Benot, L. Thiery, O. Darsonville, D. Landais, C. Piel, M. Defossez, S. Devidal, C. Escape, O. Ravel, N. Fromin, F. Volaire, A. Milcu, M. Bahn, J.-F. Soussana, Elevated CO2 maintains grassland net carbon uptake under a future heat and drought extreme. *Proc. Natl. Acad. Sci. U.S.A.* **113**, 6224–6229 (2016).

27. J. Limpens, F. Berendse, C. Blodau, J. G. Canadell, C. Freeman, J. Holden, N. Roulet, H. Rydin, G. Schaepman-Strub, Peatlands and the carbon cycle: From local processes to global implications – a synthesis. *Biogeosciences* **5**, 1475–1491 (2008).

28. P. Friedlingstein, M. O'Sullivan, M. W. Jones, R. M. Andrew, D. C. E. Bakker, J. Hauck, P. Landschützer, C. Le Quéré, I. T. Luijkx, G. P. Peters, W. Peters, J. Pongratz, C. Schwingshackl, S. Sitch, J. G. Canadell, P. Ciais, R. B. Jackson, S. R. Alin, P. Anthoni, L. Barbero, N. R. Bates, M. Becker, N. Bellouin, B. Decharme, L. Bopp, I. B. M. Brasika, P. Cadule, M. A. Chamberlain, N. Chandra, T.-T.-T. Chau, F. Chevallier, L. P. Chini, M. Cronin, X. Dou, K. Enyo, W. Evans, S. Falk, R. A. Feely, L. Feng, D. J. Ford, T. Gasser, J. Ghattas, T. Gkritzalis, G. Grassi, L. Gregor, N. Gruber, Ö. Gürses, I. Harris, M. Hefner, J. Heinke, R. A. Houghton, G. C. Hurtt, Y. Iida, T. Ilyina, A. R. Jacobson, A. Jain, T. Jarníková, A. Jersild, F. Jiang, Z. Jin, F. Joos, E. Kato, R. F. Keeling, D. Kennedy, K. Klein Goldewijk, J. Knauer, J. I. Korsbakken, A. Körtzinger, X. Lan, N. Lefèvre, H. Li, J. Liu, Z. Liu, L. Ma, G. Marland, N. Mayot, P. C. McGuire, G. A. McKinley, G. Meyer, E. J. Morgan, D. R. Munro, S.-I. Nakaoka, Y. Niwa, K. M. O'Brien, A. Olsen, A. M. Omar, T. Ono, M. Paulsen, D. Pierrot, K. Pocock, B. Poulter, C. M. Powis, G. Rehder, L. Resplandy, E. Robertson, C. Rödenbeck, T. M. Rosan, J. Schwinger, R. Séférian, T. L. Smallman, S. M. Smith, R. Sospedra-Alfonso, Q. Sun, A. J. Sutton, C. Sweeney, S. Takao, P. P. Tans, H. Tian, B. Tilbrook, H. Tsujino, F. Tubiello, G. R. van der Werf, E. van Ooijen, R. Wanninkhof, M. Watanabe, C. Wimart-Rousseau, D. Yang, X. Yang, W. Yuan, X. Yue, S. Zaehle, J. Zeng, B. Zheng, Global Carbon Budget 2023. *Earth Syst. Sci. Data* **15**, 5301–5369 (2023).

29. Z. Yu, J. Loisel, D. P. Brosseau, D. W. Beilman, S. J. Hunt, Global peatland dynamics since the Last Glacial Maximum. *Geophys. Res. Lett.* **37**, 2010GL043584 (2010).

30. E. Dorrepaal, S. Toet, R. S. P. van Logtestijn, E. Swart, M. J. van de Weg, T. V. Callaghan, R. Aerts, Carbon respiration from subsurface peat accelerated by climate warming in the subarctic. *Nature* **460**, 616–619 (2009).

31. A. L. Gill, M. A. Giasson, R. Yu, A. C. Finzi, Deep peat warming increases surface methane and carbon dioxide emissions in a black spruce-dominated ombrotrophic bog. *Glob. Chang. Biol.* **23**, 5398–5411 (2017).

32. S. Page, S. Mishra, F. Agus, G. Anshari, G. Dargie, S. Evers, J. Jauhiainen, A. Jaya, A. J. Jovani-Sancho, A. Laurén, S. Sjögersten, I. A. Suspense, L. S. Wijedasa, C. D. Evans, Anthropogenic impacts on lowland tropical peatland biogeochemistry. *Nat. Rev. Earth Environ.* **3**, 426–443 (2022).

33. IPCC, *Climate Change 2013: The Physical Science Basis. Contribution of Working Group I to the Fifth Assessment Report of the Intergovernmental Panel on Climate Change*, T. F. Stocker, D. Qin, G.-K. Plattner, M. Tignor, S. K. Allen, J. Boschung, A. Nauels, Y. Xia, V. Bex, P. M. Midgley, Eds. (Cambridge Univ. Press, 2013).

34. M. Lund, T. R. Christensen, A. Lindroth, P. Schubert, Effects of drought conditions on the carbon dioxide dynamics in a temperate peatland. *Environ. Res. Lett.* **7**, 045704 (2012).

35. J. Bubier, P. Crill, A. Mosedale, S. Frolking, E. Linder, Peatland responses to varying interannual moisture conditions as measured by automatic CO2 chambers. *Global Biogeochem. Cycles* **17**, 2002GB001946 (2003).

36. T. Ise, A. L. Dunn, S. C. Wofsy, P. R. Moorcroft, High sensitivity of peat decomposition to climate change through water-table feedback. *Nat. Geosci.* **1**, 763–766 (2008).

37. R. Garisoain, A. Jacotot, C. Delire, S. Binet, G. Le Roux, S. Gascoin, T. Rosset, S. Gogo, F. Granouillac, V. Payre-Suc, L. Gandois, Mountain Peatlands and Drought: Carbon Cycling in the Pyrenees Amidst Global Climate Change. *J. Geophys. Res. Biogeosci.* **129**, e2024JG008041 (2024).

38. C. Estop-Aragonés, K. Zając, C. Blodau, Effects of extreme experimental drought and rewetting on CO2 and CH4 exchange in mesocosms of 14 European peatlands with different nitrogen and sulfur deposition. *Glob. Chang. Biol.* **22**, 2285–2300 (2016).

39. E. A. Ainsworth, S. P. Long, 30 years of free-air carbon dioxide enrichment (FACE): What have we learned about future crop productivity and its potential for adaptation? *Glob. Chang. Biol.* **27**, 27–49 (2021).

40. N. Fenner, C. Freeman, Drought-induced carbon loss in peatlands. *Nat. Geosci.* **4**, 895–900 (2011).

41. D. Olefeldt, E. S. Euskirchen, J. Harden, E. Kane, A. D. McGuire, M. P. Waldrop, M. R. Turetsky, A decade of boreal rich fen greenhouse gas fluxes in response to natural and experimental water table variability. *Glob. Chang. Biol.* **23**, 2428–2440 (2017).

42. C. D. Evans, M. Peacock, A. J. Baird, R. R. E. Artz, A. Burden, N. Callaghan, P. J. Chapman, H. M. Cooper, M. Coyle, E. Craig, A. Cumming, S. Dixon, V. Gauci, R. P. Grayson, C. Helfter, C. M. Heppell, J. Holden, D. L. Jones, J. Kaduk, P. Levy, R. Matthews, N. P. McNamara, T. Misselbrook, S. Oakley, S. E. Page, M. Rayment, L. M. Ridley, K. M. Stanley, J. L. Williamson, F. Worrall, R. Morrison, Overriding water table control on managed peatland greenhouse gas emissions. *Nature* **593**, 548–552 (2021).

43. L. Ma, G. Zhu, B. Chen, K. Zhang, S. Niu, J. Wang, P. Ciais, H. Zuo, A globally robust relationship between water table decline, subsidence rate, and carbon release from peatlands. *Commun. Earth Environ.* **3**, 254 (2022).

44. S. Q. Wan, R. J. Norby, K. S. Pregitzer, J. Ledford, E. G. O'Neill, CO2 enrichment and warming of the atmosphere enhance both productivity and mortality of maple tree fine roots. *New Phytol.* **162**, 437–446 (2004).

45. R. B. Jackson, C. W. Cook, J. S. Pippen, S. M. Palmer, Increased belowground biomass and soil CO2 fluxes after a decade of carbon dioxide enrichment in a warm-temperate forest. *Ecology* **90**, 3352–3366 (2009).

46. C. A. Dietzen, K. S. Larsen, P. L. Ambus, A. Michelsen, M. F. Arndal, C. Beier, S. Reinsch, I. K. Schmidt, Accumulation of soil carbon under elevated CO_2 unaffected by warming and drought. *Glob. Chang. Biol.* **25**, 2970–2977 (2019).

47. J. Cui, M. Zheng, Z. Bian, N. Pan, H. Tian, X. Zhang, Z. Qiu, J. Xu, B. Gu, Elevated CO2 levels promote both carbon and nitrogen cycling in global forests. *Nat. Clim. Chang.* **14**, 511–517 (2024).

48. M. Jiang, B. E. Medlyn, J. E. Drake, R. A. Duursma, I. C. Anderson, C. V. M. Barton, M. M. Boer, Y. Carrillo, L. Castañeda-Gómez, L. Collins, K. Y. Crous, M. G. De Kauwe, B. M. Dos Santos, K. M. Emmerson, S. L. Facey, A. N. Gherlenda, T. E. Gimeno, S. Hasegawa, S. N. Johnson, A. Kännaste, C. A. Macdonald, K. Mahmud, B. D. Moore, L. Nazaries, E. H. J. Neilson, U. N. Nielsen, Ü. Niinemets, N. J. Noh, R. Ochoa-Hueso, V. S. Pathare, E. Pendall, J. Pihlblad, J. Piñeiro, J. R. Powell, S. A. Power, P. B. Reich, A. A. Renchon, M. Riegler, R. Rinnan, P. D. Rymer, R. L. Salomón, B. K. Singh, B. Smith, M. G. Tjoelker, J. K. M. Walker, A. Wujeska-Klause, J. Yang, S. Zaehle, D. S. Ellsworth, The fate of carbon in a mature forest under carbon dioxide enrichment. *Nature* **580**, 227–231 (2020).

49. N. O. E. Ofiti, M. W. I. Schmidt, S. Abiven, P. J. Hanson, C. M. Iversen, R. M. Wilson, J. E. Kostka, G. L. B. Wiesenberg, A. Malhotra, Climate warming and elevated CO_2 alter peatland soil carbon sources and stability. *Nat. Commun.* **14**, 7533 (2023).

50. R. M. Wilson, M. M. Tfaily, M. Kolton, E. R. Johnston, C. Petro, C. A. Zalman, P. J. Hanson, H. M. Heyman, J. E. Kyle, D. W. Hoyt, E. K. Eder, S. O. Purvine, R. K. Kolka, S. D. Sebestyen, N. A. Griffiths, C. W. Schadt, J. K. Keller, S. D. Bridgham, J. P. Chanton, J. E. Kostka, Soil metabolome response to whole-ecosystem warming at the Spruce and Peatland Responses under Changing Environments experiment. *Proc. Natl. Acad. Sci. U.S.A.* **118**, e2004192118 (2021).

51. S. Li, X. Li, Z. Wei, F. Liu, ABA-mediated modulation of elevated CO_2 on stomatal response to drought. *Curr. Opin. Plant Biol.* **56**, 174–180 (2020).

52. L. O. A. Abdelhakim, R. Zhou, C.-O. Ottosen, Physiological Responses of Plants to Combined Drought and Heat under Elevated CO2. *Agronomy (Basel)* **12**, 2526 (2022).

53. J. M. Warren, R. J. Norby, S. D. Wullschleger, Elevated CO_2 enhances leaf senescence during extreme drought in a temperate forest. *Tree Physiol.* **31**, 117–130 (2011).

54. M. G. De Kauwe, B. E. Medlyn, D. T. Tissue, To what extent can rising [CO_2] ameliorate plant drought stress? *New Phytol.* **231**, 2118–2124 (2021).

55. A. Asemaninejad, R. G. Thorn, B. A. Branfireun, Z. Lindo, Climate change favours specific fungal communities in boreal peatlands. *Soil Biol. Biochem.* **120**, 28–36 (2018).

56. A. M. Hopple, R. M. Wilson, M. Kolton, C. A. Zalman, J. P. Chanton, J. Kostka, P. J. Hanson, J. K. Keller, S. D. Bridgham, Massive peatland carbon banks vulnerable to rising temperatures. *Nat. Commun.* **11**, 2373 (2020).

57. L. Bragazza, J. Parisod, A. Buttler, R. D. Bardgett, Biogeochemical plant-soil microbe feedback in response to climate warming in peatlands. *Nat. Clim. Chang.* **3**, 273–277 (2013).

58. M. Helbig, T. Živković, P. Alekseychik, M. Aurela, T. S. El-Madany, E. S. Euskirchen, L. B. Flanagan, T. J. Griffis, P. J. Hanson, J. Hattakka, C. Helfter, T. Hirano, E. R. Humphreys, G. Kiely, R. K. Kolka, T. Laurila, P. G. Leahy, A. Lohila, I. Mammarella, M. B. Nilsson, A. Panov, F. J. W. Parmentier, M. Peichl, J. Rinne, D. T. Roman, O. Sonnentag, E.-S. Tuittila, M. Ueyama, T. Vesala, P. Vestin, S. Weldon, P. Weslien, S. Zaehle, Warming response of peatland CO2 sink is sensitive to seasonality in warming trends. *Nat. Clim. Chang.* **12**, 743–749 (2022).

59. A. Volder, R. M. Gifford, J. R. Evans, Effects of elevated atmospheric CO_2, cutting frequency, and differential day/night atmospheric warming on root growth and turnover of *Phalaris* swards. *Glob. Change Biol.* **13**, 1040–1052 (2007).

60. K. Meeran, J. Ingrisch, D. Reinthaler, A. Canarini, L. Müller, E. M. Pötsch, A. Richter, W. Wanek, M. Bahn, Warming and elevated CO_2 intensify drought and recovery responses of grassland carbon allocation to soil respiration. *Glob. Chang. Biol.* **27**, 3230–3243 (2021).

61. A. Malhotra, D. J. Brice, J. Childs, J. D. Graham, E. A. Hobbie, H. Vander Stel, S. C. Feron, P. J. Hanson, C. M. Iversen, Peatland warming strongly increases fine-root growth. *Proc. Natl. Acad. Sci. U.S.A.* **117**, 17627–17634 (2020).

62. R. M. Wilson, A. M. Hopple, M. M. Tfaily, S. D. Sebestyen, C. W. Schadt, L. Pfeifer-Meister, C. Medvedeff, K. J. McFarlane, J. E. Kostka, M. Kolton, R. K. Kolka, L. A. Kluber, J. K. Keller, T. P. Guilderson, N. A. Griffiths, J. P. Chanton, S. D. Bridgham, P. J. Hanson, Stability of peatland carbon to rising temperatures. *Nat. Commun.* **7**, 13723 (2016).

63. O. C. Calvo, J. Franzaring, I. Schmid, M. Müller, N. Brohon, A. Fangmeier, Atmospheric CO_2 enrichment and drought stress modify root exudation of barley. *Glob. Chang. Biol.* **23**, 1292–1304 (2017).

64. L. Xiong, X. Liu, G. Vinci, B. Sun, M. Drosos, L. Li, A. Piccolo, G. Pan, Aggregate fractions shaped molecular composition change of soil organic matter in a rice paddy under elevated CO2 and air warming. *Soil Biol. Biochem.* **159**, 108289 (2021).

65. Y. Carrillo, F. Dijkstra, D. LeCain, D. Blumenthal, E. Pendall, Elevated CO_2 and warming cause interactive effects on soil carbon and shifts in carbon use by bacteria. *Ecol. Lett.* **21**, 1639–1648 (2018).

66. N. O. E. Ofiti, E. F. Solly, P. J. Hanson, A. Malhotra, G. L. B. Wiesenberg, M. W. I. Schmidt, Warming and elevated CO_2 promote rapid incorporation and degradation of plant-derived organic matter in an ombrotrophic peatland. *Glob. Chang. Biol.* **28**, 883–898 (2022).

67. S. Frolking, J. Talbot, M. C. Jones, C. C. Treat, J. B. Kauffman, E.-S. Tuittila, N. Roulet, Peatlands in the Earth's 21st century climate system. *Environ. Rev.* **19** (NA), 371–396 (2011).

68. S. E. Ward, N. J. Ostle, S. Oakley, H. Quirk, P. A. Henrys, R. D. Bardgett, Warming effects on greenhouse gas fluxes in peatlands are modulated by vegetation composition. *Ecol. Lett.* **16**, 1285–1293 (2013).

69. A. V. Gallego-Sala, D. J. Charman, S. Brewer, S. E. Page, I. C. Prentice, P. Friedlingstein, S. Moreton, M. J. Amesbury, D. W. Beilman, S. Björck, T. Blyakharchuk, C. Bochicchio, R. K. Booth, J. Bunbury, P. Camill, D. Carless, R. A. Chimner, M. Clifford, E. Cressey, C. Courtney-Mustaphi, F. De Vleeschouwer, R. de Jong, B. Fialkiewicz-Koziel, S. A. Finkelstein, M. Garneau, E. Githumbi, J. Hribjlan, J. Holmquist, P. D. M. Hughes, C. Jones, M. C. Jones, E. Karofeld, E. S. Klein, U. Kokfelt, A. Korhola, T. Lacourse, G. Le Roux, M. Lamentowicz, D. Large, M. Lavoie, J. Loisel, H. Mackay, G. M. MacDonald, M. Makila, G. Magnan, R. Marchant, K. Marcisz, A. Martínez Cortizas, C. Massa, P. Mathijssen, D. Mauquoy, T. Mighall, F. J. G. Mitchell, P. Moss, J. Nichols, P. O. Oksanen, L. Orme, M. S. Packalen, S. Robinson, T. P. Roland, N. K. Sanderson, A. B. K. Sannel, N. Silva-Sánchez, N. Steinberg, G. T. Swindles, T. E. Turner, J. Uglow, M. Väliranta, S. van Bellen, M. van der Linden, B. van Geel, G. Wang, Z. Yu, J. Zaragoza-Castells, Y. Zhao, Latitudinal limits to the predicted increase of the peatland carbon sink with warming. *Nat. Clim. Chang.* **8**, 907–913 (2018).

70. P. J. Hanson, N. A. Griffiths, C. M. Iversen, R. J. Norby, S. D. Sebestyen, J. R. Phillips, J. P. Chanton, R. K. Kolka, A. Malhotra, K. C. Oleheiser, J. M. Warren, X. Shi, X. Yang, J. Mao, D. M. Ricciuto, Rapid Net Carbon Loss From a Whole-Ecosystem Warmed Peatland. *AGU Adv.* **1**, e2020AV000163 (2020).

71. N. A. Griffiths, P. J. Hanson, D. M. Ricciuto, C. M. Iversen, A. M. Jensen, A. Malhotra, K. J. McFarlane, R. J. Norby, K. Sargsyan, S. D. Sebestyen, X. Shi, A. P. Walker, E. J. Ward, J. M. Warren, D. J. Weston, Temporal and Spatial Variation in Peatland Carbon Cycling and Implications for Interpreting Responses of an Ecosystem-Scale Warming Experiment. *Soil Sci. Soc. Am. J.* **81**, 1668–1688 (2017).

72. Z. C. Yu, Northern peatland carbon stocks and dynamics: A review. *Biogeosciences* **9**, 4071–4085 (2012).

73. H. Chen, X. Xu, C. Fang, B. Li, M. Nie, Differences in the temperature dependence of wetland CO2 and CH4 emissions vary with water table depth. *Nat. Clim. Chang.* **11**, 766–771 (2021).

74. Y. Huang, P. Ciais, Y. Luo, D. Zhu, Y. Wang, C. Qiu, D. S. Goll, B. Guenet, D. Makowski, I. De Graaf, J. Leifeld, M. J. Kwon, J. Hu, L. Qu, Tradeoff of CO2 and CH4 emissions from global peatlands under water-table drawdown. *Nat. Clim. Chang.* **11**, 618–622 (2021).

75. A. Günther, A. Barthelmes, V. Huth, H. Joosten, G. Jurasinski, F. Koebsch, J. Couwenberg, Prompt rewetting of drained peatlands reduces climate warming despite methane emissions. *Nat. Commun.* **11**, 1644 (2020).

76. Q. Quan, J. Zhou, P. J. Hanson, D. Ricciuto, S. D. Sebestyen, D. J. Weston, J. P. Chanton, R. M. Wilson, J. E. Kostka, Y. Zhou, N. Wei, L. Jiang, M. A. Mayes, J. M. Stelling, A. D. Richardson, M. E. Dusenge, D. Way, J. M. Warren, Y. Luo, Drought-induced peatland carbon loss exacerbated by elevated CO_2 and warming. figshare (2024); https://doi.org/10.6084/m9.figshare.27857655.

77. Oak Ridge National Laboratory, SPRUCE: Spruce and Peatland Responses Under Changing Environments. https://mnspruce.ornl.gov/ (n.d.).

78. S. D. Sebestyen, C. Dorrance, D. M. Olson, E. S. Verry, R. K. Kolka, A. E. Elling, R. Kyllander, “Long-term monitoring sites and trends at the Marcell Experimental Forest” in *Peatland Biogeochemistry and Watershed Hydrology at the Marcell Experimental Forest*, R. Kolka, S. Sebestyen, E. S. Verry, K. Brooks, Eds. (CRC Press, 2011), pp. 15–71.

79. S. D. Sebestyen, E. S. Verry, A. E. Elling, R. L. Kyllander, D. T. Roman, J. M. Burdick, N. K. Lany, R. K. Kolka, Marcell Experimental Forest daily precipitation, 1961 - ongoing, Forest Service Research Data Archive (2020); https://doi.org/10.2737/RDS-2020-0062.

80. P. J. Hanson, J. S. Riggs, W. R. Nettles, J. R. Phillips, M. B. Krassovski, L. A. Hook, L. Gu, A. D. Richardson, D. M. Aubrecht, D. M. Ricciuto, J. M. Warren, C. Barbier, Attaining whole-ecosystem warming using air and deep-soil heating methods with an elevated CO2 atmosphere. *Biogeosciences* **14**, 861–883 (2017).

81. A. L. Healey, B. Piatkowski, J. T. Lovell, A. Sreedasyam, S. B. Carey, S. Mamidi, S. Shu, C. Plott, J. Jenkins, T. Lawrence, B. Aguero, A. A. Carrell, M. Nieto-Lugilde, J. Talag, A. Duffy, S. Jawdy, K. R. Carter, L.-B. Boston, T. Jones, J. Jaramillo-Chico, A. Harkess, K. Barry, K. Keymanesh, D. Bauer, J. Grimwood, L. Gunter, J. Schmutz, D. J. Weston, A. J. Shaw, Newly identified sex chromosomes in the Sphagnum (peat moss) genome alter carbon sequestration and ecosystem dynamics. *Nat. Plants* **9**, 238–254 (2023).

82. A. D. Parsekian, L. Slater, D. Ntarlagiannis, J. Nolan, S. D. Sebesteyen, R. K. Kolka, P. J. Hanson, Uncertainty in Peat Volume and Soil Carbon Estimated Using Ground-Penetrating Radar and Probing. *Soil Sci. Soc. Am. J.* **76**, 1911–1918 (2012).

83. K. J. McFarlane, P. J. Hanson, C. M. Iversen, J. R. Phillips, D. J. Brice, Local Spatial Heterogeneity of Holocene Carbon Accumulation throughout the Peat Profile of an Ombrotrophic Northern Minnesota Bog. *Radiocarbon* **60**, 941–962 (2018).

84. P. J. Hanson, J. S. Riggs, W. R. Nettles, M. B. Krassovski, L. A. Hook, SPRUCE Whole Ecosystems Warming (WEW) Environmental Data Beginning August, 2015, Oak Ridge National Laboratory, TES SFA, U.S. Department of Energy (2016); https://doi.org/10.3334/CDIAC/spruce.032.

85. P. J. Hanson, A. L. Gill, X. Xu, J. R. Phillips, D. J. Weston, R. K. Kolka, J. S. Riggs, L. A. Hook, Intermediate-scale community-level flux of CO2 and CH4 in a Minnesota peatland: Putting the SPRUCE project in a global context. *Biogeochemistry* **129**, 255–272 (2016).

86. S. B. Hodgkins, C. J. Richardson, R. Dommain, H. Wang, P. H. Glaser, B. Verbeke, B. R. Winkler, A. R. Cobb, V. I. Rich, M. Missilmani, N. Flanagan, M. Ho, A. M. Hoyt, C. F. Harvey, S. R. Vining, M. A. Hough, T. R. Moore, P. J. H. Richard, F. B. De La Cruz, J. Toufaily, R. Hamdan, W. T. Cooper, J. P. Chanton, Tropical peatland carbon storage linked to global latitudinal trends in peat recalcitrance. *Nat. Commun.* **9**, 3640 (2018).

87. M. R. Baysinger, R. M. Wilson, P. J. Hanson, J. E. Kostka, J. P. Chanton, Compositional stability of peat in ecosystem-scale warming mesocosms. *PLOS ONE* **17**, e0263994 (2022).

88. M. R. Baysinger, R. M. Wilson, P. J. Hanson, J. E. Kostka, J. P. Chanton, SPRUCE: Compositional Stability of Peat in Ecosystem-Scale Warming Mesocosms, 2014 and

2019, Oak Ridge National Laboratory, TES SFA, U.S. Department of Energy (2021); https://doi.org/10.25581/spruce.093/1820162.

89. D. A. Merritt, J. M. Hayes, D. J. Des Marais, Carbon isotopic analysis of atmospheric methane by isotope-ratio-monitoring gas chromatography-mass spectrometry. *J. Geophys. Res.* **100** (D1), 1317–1326 (1995).

90. R. Wilson, M. M. Tfaily, M. M. Kolton, E. Johnston, C. Petro, C. M. Zalman, P. J. Hanson, H. M. Heyman, J. Kyle, D. W. Hoyt, E. K. Eder, S. O. Purvine, R. K. Kolka, S. D. Sebestyen, N. A. Griffiths, C. W. Schadt, J. K. Keller, S. D. Bridgham, J. P. Chanton, J. E. Kostka, SPRUCE: Soil Metabolome Responses to Whole Ecosystem Warming in SPRUCE Experimental Plots Beginning in 2016, Oak Ridge National Laboratory, TES SFA, U.S. Department of Energy (2021); https://doi.org/10.25581/spruce.083/1647173.

91. R. J. Norby, J. Childs, SPRUCE: Sphagnum Productivity and Community Composition in the SPRUCE Experimental Plots, Oak Ridge National Laboratory, TES SFA, U.S. Department of Energy (2018); https://doi.org/10.25581/spruce.049/1426474.

92. R. J. Norby, J. Childs, P. J. Hanson, J. M. Warren, Rapid loss of an ecosystem engineer: *Sphagnum* decline in an experimentally warmed bog. *Ecol. Evol.* **9**, 12571–12585 (2019).

93. S. D. Sebestyen, E. S. Verry, A.E. Elling, R. L. Kyllander, D. T. Roman, J. M. Burdick, N. K. Lany, R. K. Kolka, Marcell Experimental Forest daily peatland water table elevation. 1961 - ongoing ver 1963, Environmental Data Initiative, Forest Service Research Data Archive (2024); https://doi.org/10.2737/RDS-2018-0002-2.

94. P. Calanca, Climate change and drought occurrence in the Alpine region: How severe are becoming the extremes? *Global Planet. Change* **57**, 151–160 (2007).

95. IPCC, *Climate Change 2014: Synthesis Report. Contribution of Working Groups I, II and III to the Fifth Assessment Report of the Intergovernmental Panel on Climate Change*, Core Writing Team, R. K. Pachauri, L. A. Meyer, Eds. (IPCC, 2014).

96. P. J. Hanson, J. R. Phillips, J. S. Riggs, W. R. Nettles, D. E. Todd, SPRUCE Large-Collar In Situ CO2 and CH4 Flux Data for the SPRUCE Experimental Plots, Carbon Dioxide Information Analysis Center, Oak Ridge National Laboratory, U.S. Department of Energy (2014); http://dx.doi.org/10.3334/CDIAC/spruce.006.

97. J. M. Stelling, M. A. Mayes, P. J. Hanson, M. Krassovski, SPRUCE: Carbon Dioxide and Methane Soil Flux Measurements at High Temporal Resolution, Beginning in 2022, Oak Ridge National Laboratory, TES SFA, U.S. Department of Energy (2024); https://doi.org/10.25581/spruce.104/1922635.

98. M. Kuhn, Building predictive models in R using the caret package. *J. Stat. Softw.* **28**, 1–26 (2008).

99. L. Breiman, Random forests. *Mach. Learn.* **45**, 5–32 (2001).

100. D. I. Warton, I. J. Wright, D. S. Falster, M. Westoby, Bivariate line-fitting methods for allometry. *Biol. Rev. Camb. Philos. Soc.* **81**, 259–291 (2006).

101. A. A. Correndo, T. J. Hefley, D. P. Holzworth, I. A. Ciampitti, Revisiting linear regression to test agreement in continuous predicted-observed datasets. *Agric. Syst.* **192**, 103194 (2021).

102. J. V. Tavares, R. S. Oliveira, M. Mencuccini, C. Signori-Müller, L. Pereira, F. C. Diniz, M. Gilpin, M. J. Marca Zevallos, C. A. Salas Yupayccana, M. Acosta, F. M. Pérez Mullisaca, F. V. Barros, P. Bittencourt, H. Jancoski, M. C. Scalon, B. S. Marimon, I. Oliveras Menor, B. H. Marimon Jr., M. Fancourt, A. Chambers-Ostler, A. Esquivel-Muelbert, L. Rowland, P. Meir, A. C. Lola da Costa, A. Nina, J. M. B. Sanchez, J. S. Tintaya, R. S. C. Chino, J. Baca, L. Fernandes, E. R. M. Cumapa, J. A. R. Santos, R. Teixeira, L. Tello, M. T. M. Ugarteche, G. A. Cuellar, F. Martinez, A. Araujo-Murakami, E. Almeida, W. J. A. da Cruz, J. Del Aguila Pasquel, L. Aragão, T. R. Baker, P. B. de Camargo, R. Brienen, W. Castro, S. C. Ribeiro, F. Coelho de Souza, E. G. Cosio, N. Davila Cardozo, R. da Costa Silva, M. Disney, J. S. Espejo, T. R. Feldpausch, L. Ferreira, L. Giacomin, N. Higuchi, M. Hirota, E. Honorio, W. Huaraca Huasco, S. Lewis, G. Flores Llampazo, Y. Malhi, A. Monteagudo Mendoza, P. Morandi, V. Chama Moscoso, R. Muscarella, D. Penha, M. C. Rocha, G. Rodrigues, A. R. Ruschel, N. Salinas, M. Schlickmann, M. Silveira, J. Talbot, R. Vásquez, L. Vedovato, S. A. Vieira, O. L. Phillips, E. Gloor, D. R. Galbraith, Basin-wide variation in tree hydraulic safety margins predicts the carbon balance of Amazon forests. *Nature* **617**, 111–117 (2023).

103. E. C. Fricke, J.-C. Svenning, Accelerating homogenization of the global plant-frugivore meta-network. *Nature* **585**, 74–78 (2020).

104. D. I. Warton, R. A. Duursma, D. S. Falster, S. Taskinen, smatr 3– an R package for estimation and inference about allometric lines. *Methods Ecol. Evol.* **3**, 257–259 (2012).

105. P. J. Hanson, J. R. Phillips, S. D. Wullschleger, W. R. Nettles, J. M. Warren, E. J. Ward, J. D. Graham, T. A. Ruggles, SPRUCE Tree Growth Assessments of Picea and Larix in S1-Bog Plots and SPRUCE Experimental Plots beginning in 2011, Version 2. Oak Ridge National Laboratory, TES SFA, U.S. Department of Energy (2018); https://doi.org/10.25581/spruce.051/1433836.

106. P. J. Hanson, D. Brice, C. T. Garten, L. A. Hook, J. Phillips, D. E. Todd, SPRUCE S1 Bog Vegetation Allometric and Biomass Data: 2010-2011. Oak Ridge National Laboratory, TES SFA, U.S. Department of Energy (2012); https://doi.org/10.3334/CDIAC/spruce.004.

107. E. Weng, Y. Luo, Soil hydrological properties regulate grassland ecosystem responses to multifactor global change: A modeling analysis. *J. Geophys. Res. Biogeosci.* **113**, 3003 (2008).

108. S. Ma, J. Jiang, Y. Huang, Z. Shi, R. M. Wilson, D. Ricciuto, S. D. Sebestyen, P. J. Hanson, Y. Luo, Data-Constrained Projections of Methane Fluxes in a Northern Minnesota Peatland in Response to Elevated CO2 and Warming. *J. Geophys. Res. Biogeosci.* **122**, 2841–2861 (2017).

109. G. D. Farquhar, S. von Caemmerer, J. A. Berry, A biochemical model of photosynthetic CO2 assimilation in leaves of C 3 species. *Planta* **149**, 78–90 (1980).

110. J. T. Ball, I. E. Woodrow, J. A. Berry, in *Progress in Photosynthesis Research: Volume 4 Proceedings of the VIIth International Congress on Photosynthesis Providence, Rhode Island, USA, August 10–15, 1986*, J. Biggins, Ed. (Springer Netherlands, 1987), pp. 221–224.

111. Y. P. Wang, R. Leuning, A two-leaf model for canopy conductance, photosynthesis and partitioning of available energy I: Model description and comparison with a multi-layered model. *Agric. For. Meteorol.* **91**, 89–111 (1998).

112. S. Ma, L. Jiang, R. M. Wilson, J. Chanton, S. Niu, C. M. Iversen, A. Malhotra, J. Jiang, Y. Huang, X. Lu, Z. Shi, F. Tao, J. Liang, D. Ricciuto, P. J. Hanson, Y. Luo, Thermal acclimation of plant photosynthesis and autotrophic respiration in a northern peatland. *Environ. Res. Clim.* **2**, 025003 (2023).

113. T. Xu, L. White, D. Hui, Y. Luo, Probabilistic inversion of a terrestrial ecosystem model: Analysis of uncertainty in parameter estimation and model prediction. *Global Biogeochem. Cycles* **20**, 2005GB002468 (2006).

114. F. Tao, Y. Huang, B. A. Hungate, S. Manzoni, S. D. Frey, M. W. I. Schmidt, M. Reichstein, N. Carvalhais, P. Ciais, L. Jiang, J. Lehmann, Y.-P. Wang, B. Z. Houlton, B. Ahrens, U. Mishra, G. Hugelius, T. D. Hocking, X. Lu, Z. Shi, K. Viatkin, R. Vargas, Y. Yigini, C. Omuto, A. A. Malik, G. Peralta, R. Cuevas-Corona, L. E. Di Paolo, I. Luotto, C. Liao, Y.-S. Liang, V. S. Saynes, X. Huang, Y. Luo, Microbial carbon use efficiency promotes global soil carbon storage. *Nature* **618**, 981–985 (2023).

115. M. E. Dusenge, E. J. Ward, J. M. Warren, D. A. McLennan, J. R. Stinziano, B. K. Murphy, A. W. King, J. Childs, D. J. Brice, J. R. Phillips, A. Stefanski, R. Villanueva, S. D. Wullschleger, M. Cruz, P. B. Reich, D. A. Way, SPRUCE Photosynthesis and Respiration of *Picea mariana* and *Larix laricina* in SPRUCE Experimental Plots, 2016-2017, Oak Ridge National Laboratory, TES SFA, U.S. Department of Energy (2021); https://doi.org/10.25581/spruce.056/1455138.

116. M. E. Dusenge *et al*., SPRUCE Photosynthesis and Respiration of *Picea mariana* and *Larix laricina* in SPRUCE Experimental Plots, 2019, Oak Ridge National Laboratory, TES SFA, U.S. Department of Energy (2025).

117. A. D. Richardson, K. Hufkens, T. Milliman, D. M. Aubrecht, M. E. Furze, B. Seyednasrollah, M. B. Krassovski, J. M. Latimer, W. R. Nettles, R. R. Heiderman, J. M. Warren, P. J. Hanson, Ecosystem warming extends vegetation activity but heightens vulnerability to cold temperatures. *Nature* **560**, 368–371 (2018).

118. J. Wu, L. P. Albert, A. P. Lopes, N. Restrepo-Coupe, M. Hayek, K. T. Wiedemann, K. Guan, S. C. Stark, B. Christoffersen, N. Prohaska, J. V. Tavares, S. Marostica, H. Kobayashi, M. L. Ferreira, K. S. Campos, R. da Silva, P. M. Brando, D. G. Dye, T. E. Huxman, A. R. Huete, B. W. Nelson, S. R. Saleska, Leaf development and demography explain photosynthetic seasonality in Amazon evergreen forests. *Science* **351**, 972–976 (2016).

119. T. B. Brown, K. R. Hultine, H. Steltzer, E. G. Denny, M. W. Denslow, J. Granados, S. Henderson, D. Moore, S. Nagai, M. SanClements, A. Sánchez-Azofeifa, O. Sonnentag, D. Tazik, A. D. Richardson, Using phenocams to monitor our changing Earth: Toward a global phenocam network. *Front. Ecol. Environ.* **14**, 84–93 (2016).

120. A. D. Richardson, C. Schädel, J. Blais, T. Milliman, K. J. Pearson, M. B. Krassovski, P. J. Hanson, SPRUCE Vegetation Phenology in Experimental Plots from Phenocam Imagery, 2015-2022, Oak Ridge National Laboratory, TES SFA, U.S. Department of Energy (2021); https://doi.org/10.25581/spruce.108/1996813.

121. J. Järveoja, M. B. Nilsson, M. Gažovič, P. M. Crill, M. Peichl, Partitioning of the net CO_2 exchange using an automated chamber system reveals plant phenology as key control of production and respiration fluxes in a boreal peatland. *Glob. Chang. Biol.* **24**, 3436–3451 (2018).

122. A. Kassambara, rstatix: Pipe-friendly framework for basic statistical tests (CRAN: Contributed Packages, 2019).

123. J. Fox, S. Weisberg, *An R Companion to Applied Regression* (Sage, ed. 3, 2019).

124. E. Cule, S. Moritz, D. Frankowski, ridge: Ridge Regression with Automatic Selection of the Penalty Parameter. R package version 3.3 (2022).